Indium nitride (InN): A review on growth, characterization and properties

APPLIED PHYSICS REVIEWS—FOCUSED REVIEW

Indium nitride (InN): A review on growth, characterization, and properties

Ashraful Ghani Bhuiyan, Akihiro Hashimoto, and Akio Yamamoto[a)]
Department of Electrical & Electronics Engineering, Faculty of Engineering, Fukui University, Bunkyo 3-9-1, Fukui 910-8507, Japan

(Received 2 February 2003; accepted 28 April 2003)

During the last few years the interest in the indium nitride (InN) semiconductor has been remarkable. There have been significant improvements in the growth of InN films. High quality single crystalline InN film with two-dimensional growth and high growth rate are now routinely obtained. The background carrier concentration and Hall mobility have also improved. Observation of strong photoluminescence near the band edge is reported very recently, leading to conflicts concerning the exact band gap of InN. Attempts have also been made on the deposition of InN based heterostructures for the fabrication of InN based electronic devices. Preliminary evidence of two-dimensional electron gas accumulation in the InN and studies on InN-based field-effect transistor structure are reported. In this article, the work accomplished in the InN research, from its evolution to till now, is reviewed. The In containing alloys or other nitrides (AlGaInN, GaN, AlN) are not discussed here. We mainly concentrate on the growth, characterization, and recent developments in InN research. The most popular growth techniques, metalorganic vapor phase epitaxy and molecular beam epitaxy, are discussed in detail with their recent progress. Important phenomena in the epitaxial growth of InN as well as the problems remaining for future study are also discussed. © *2003 American Institute of Physics.* [DOI: 10.1063/1.1595135]

TABLE OF CONTENTS

[a)]Author to whom correspondence should be addressed; electronic mail: yamamoto@kyomu1.fuee.fukui-u.ac.jp

I. INTRODUCTION

A. Introductory remarks

Developments in the field of III-nitride (InN, GaN, and AlN) semiconductors have been spectacular due to their highly attractive inherent properties. During the last few years the interest in the InN has been remarkable. Recent results indicate that the InN films almost meet the requirements for application to practical devices. Many review papers and books have been published on the properties of III–nitride semiconductors and on the devices fabricated using them.[1] In most of these publications the main topic was GaN and its alloys. In recent years, the number of publications concerning InN research has increased significantly. In this article, the work accomplished in the InN research, from its evolution until now, is reviewed. We mainly concentrate on the growth, characterization, and recent development in the InN research. Important phenomena in the epitaxial growth of InN as well as the problems remaining for future study are covered. The most popular growth techniques, metalorganic vapor phase epitaxy (MOVPE) and molecular beam epitaxy (MBE), are discussed in detail with their recent progress, with the differences between film qualities grown by these techniques.

B. Important properties of InN

The development in blue/UV light emitting diodes (LEDs) and laser diodes (LDs), and also high-frequency transistors operating at high powers and temperatures,[1–4] has proved the benefits of the nitride materials system. Indium nitride (InN) is an important III-nitride semiconductor with many potential applications. The use of InN and its alloys with GaN and AlN makes it possible to extend the emission of nitride-based LEDs from ultraviolet to near infrared region. For example, along with GaN, the InN ternary alloy, InGaN, has found application in a variety of heterostructure based optoelectronic devices, such as LEDs[5,6] and lasers.[7] The InGaN quantum wells are indispensable for light emitting devices because incorporation of small concentrations of In in the active GaN layer increases luminescence efficiency considerably. InN was predicted to have lowest effective mass for electrons in all the III–nitride semiconductors,[3] which leads to high mobility and high saturation velocity. The theoretical maximum mobility calculated in InN and GaN at 300 K are about 4400 and 1000 $cm^2 V^{-1} S^{-1}$, respectively, while at 77 K the limits are beyond 30 000 and 6000 $cm^2 V^{-1} S^{-1}$, respectively.[8] The electron transport in wurtzite InN was studied using an ensemble Monte Carlo method.[9–11] It was found that InN exhibits an extremely high peak drift velocity at room temperature. The saturation velocity is much larger than that of gallium arsenide (GaAs) and gallium nitride (GaN). Figure 1 shows the velocity–field characteristics associated with wurtzite GaN, InN, AlN, and zincblende GaAs. The critical field at which the peak drift velocity was achieved for each velocity–field characteristic is clearly marked. It can be seen that each of these III–V semiconductors achieves a peak in its velocity–field characteristic. InN achieves the highest steady-state peak drift velocity: 4.2×10^7 cm/s. This contrasts with the case of GaN,

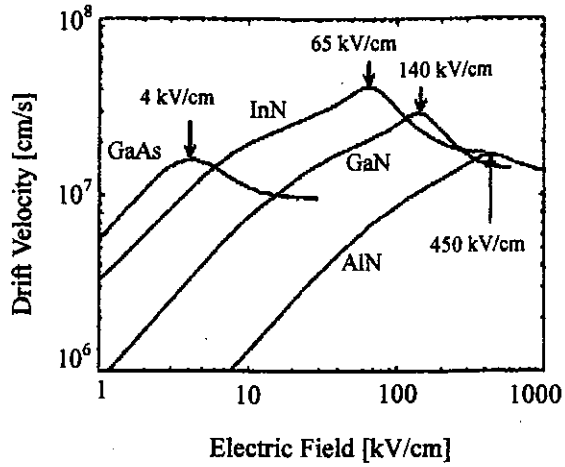

FIG. 1. The velocity–field characteristics associated with wurtzite GaN, InN, AlN, and zincblende GaAs. In all cases, the temperature was set to 300 K and the doping concentration was set to 10^{17} cm^{-3}. The critical field at which the peak drift velocity was achieved for each velocity–field characteristic is clearly marked; 140 kV/cm for GaN, 65 kV/cm for InN, 450 kV/cm for AlN, and 4 kV/cm for GaAs (Ref. 11).

2.9×10^7 cm/s, AlN, 1.7×10^7 cm/s, and of GaAs, 1.6×10^7 cm/s. It was concluded that the transport characteristics of InN are superior to those of GaN and GaAs, over a wide range of temperature from 150 to 500 K and a doping concentration up to 10^{19} cm^{-3}.[10] The transport characteristics were shown to be relatively insensitive to variations in temperature and doping concentration, unlike GaAs. This suggests that there may be distinct advantages offered by using InN in high frequency centimeter and millimeter wave devices. The transient electron transport, which is expected to be the dominant transport mechanism in submicron-scale devices, was also studied in InN.[11] It is found that InN exhibits the highest peak overshoot velocity and that this velocity overshoot lasts over the longest distance when compared with GaN and AlN. It was predicted that InN-based field-effect transistors (FETs) have an extremely high speed with a cutoff frequency of over 1 THz for 0.1 μm gates. Thus, InN is a highly potential material for the fabrication of high-speed high-performance heterojunction FETs.

The most commonly quoted band gap value for InN is 1.89 eV at room temperature.[12] The LEDs, laser diodes (LDs), and transistors typically involve InGaN, with low In fractions. However, there would be great advantages in being able to incorporate large fraction of In in various applications. For example, the use of wurtzitic InN would permit photonic devices in the red and much faster electronic devices, because of higher mobility and peak velocity than those of most other III–nitride materials. The use of InN-based optoelectronic devices offers the potential of an environmental-friendly red emitter with no toxic element, which may replace GaAs-based devices. In addition, InN is a potential material for low cost solar cells with high efficiency. Yamamoto *et al.* proposed InN for a top cell material of a two-junction tandem solar cell.[13] The combination of band gap, 1.9 eV for InN and 1.1 eV for Si, is around the optimum to obtain a conversion efficiency of over 30%. The InN/Si system as a solar cell material has advantages that it

contains no poisonous elements such as arsenic and needs no toxic gases such as phosphine in the fabrication process. Qian *et al.* recently showed InN as a good plasma filter material for the widely used GaSb and GaInAsSb photovoltaic cells in thermophotovoltaic system, which show good performance.[14]

Recently, several groups studied the photoluminescence (PL) spectra of single crystalline InN and reported that the band gap energy of InN is much smaller than 1.89 eV.[15–22] They reported the band gap to be around 0.65–0.90 eV, which has created an exciting ambiguity about the exact band gap energy. These studies were carried out on the high quality InN film grown by the modern growth techniques, MOVPE and MBE, and also these are the first reports about the observation of PL in InN. These newly reported small band gap values are compatible with the wavelength of the optical fiber. Therefore, if high quality InN films with a direct band gap of 0.65–0.90 eV can be grown, it will have very important potential to fabricate high speed LDs and photodiodes (PDs) in the optical communication system which can replace the conventional semiconductor technology.

C. Evolution of InN and current progress

The first attempt to synthesize InN was made by Juza and Hahn in 1938.[23] They obtained InN from $InF_6(NH_4)_3$ and reported the crystal structure of InN to be wurtzite. After that, several attempts were made to synthesize InN by Juza and Rabenua in 1956,[24] Renner in 1958,[25] Pastrnak and Souckova in 1963,[26] Samsonov in 1969.[27] It was pointed out that direct interaction of metallic indium and nitrogen in an inactivated form does not take place even at rather high temperatures.[28] McChesney *et al.* reported that the dissociation pressure of InN is extremely high and InN is not formed by direct reaction of N_2 molecules and indium.[29] In all of the above methods, interaction of indium compound with ammonia or thermal decomposition of the complex compound containing In and N was used, and the prepared InN was in the form of powder or small crystals. The earliest success in the growth of InN with some good electrical properties was obtained by Hovel and Cuomo in 1972.[30] Polycrystalline InN film with highly preferred orientation was grown on sapphire and silicon substrates at 25–600 °C by reactive rf sputtering. The InN grown film was dark red with a resistivity in the range of $(3-5)\times10^{-3}\,\Omega\,\mathrm{cm}$, Hall mobility of $250\pm50\,\mathrm{cm^2/V\,s}$, and n-type carrier concentration of $(5-8)\times10^{18}\,\mathrm{cm^{-3}}$. In 1974, Trainor and Rose reported some properties (optical and electrical) of InN films grown on sapphire by reactive evaporation and also discussed the thermal stability of InN.[31] They found the fundamental band edge energy to be 1.7 eV and that InN is a direct band gap semiconductor. Their annealing study suggested that high atomic nitrogen pressure during the growth is fundamental to growing stoichiometric material. In that period, the growth of InN was also carried out by Andreeyva and Eliseejva[32] using sputtering and Osamura *et al.*[33,34] using electron beam plasma techniques. Osamura *et al.* synthesized the alloy of InN and GaN over the entire composition region. They measured the direct energy gap of InN to be 1.95 eV at room temperature and to be 2.11 eV at 78 K. Their samples were polycrystalline and confirmed to be n type from the observation of the thermoelectric effect. Puychevrier and Menoret reported a direct energy gap of 2.07 eV at room temperature and of 2.21 eV at 77 K for the InN film grown by reactive cathodic sputtering in 1976.[35]

Marasina *et al.* grew epitaxial layers of InN on quartz and sapphire substrates by a chemical vapor deposition method using the interaction of $InCl_3$ and NH_3.[36] The InN epitaxial layer was mosaic and n type with electron concentration of $2\times10^{20}-8\times10^{21}\,\mathrm{cm^{-3}}$ and mobility of $50-30\,\mathrm{cm^2/V\,s}$. They clarified that substrate temperature is the most important for determining the optimum growth condition, with rapid dissociation of InN occurring above 600 °C, and there was no deposition of InN layer at 670 °C at all. In the 1980s, some important works were accomplished for the growth of InN, mainly by sputtering, and the growth mechanism of InN was clarified as well.[12,37–47] Many properties of the grown InN films were studied in that period where the work of Tansley and Foley was prominent.[12,38–42] For instance, the room temperature highest mobility and lowest background carrier concentration in the InN film ($2700\,\mathrm{cm^2/V\,s}$ and $5\times10^{16}\,\mathrm{cm^{-3}}$) reported to date was grown by Tansley and Foley using radio frequency (rf) sputtering in 1984.[38]

The beginning of the single crystalline epitaxial InN film by the most popular growth technique, MOVPE, was made by Matsuoka *et al.* and Wakahara *et al.* in 1989.[48–50] Single crystalline InN films were grown on sapphire substrates by reacting trimethylindium (TMI) with NH_3 and microwave activated N_2, respectively. Epitaxial growth of single crystalline and good quality InN films was widely studied in the 1990s. These studies included growth by MOVPE and MBE on different substrates and underlying layers over a wide range of growth conditions. A remarkable improvement in the growth of InN films has been produced by MOVPE as well as MBE. The highest mobility and lowest background carrier concentration are $730\,\mathrm{cm^2/V\,s}$ and $5.8\times10^{18}\,\mathrm{cm^{-3}}$, respectively, in MOVPE grown InN.[51] The reported highest mobility in the MBE grown thick InN film is $2050\,\mathrm{cm^2/V\,s}$ and the lowest background carrier concentration is $3.49\times10^{17}\,\mathrm{cm^{-3}}$,[52] which are better than the MOVPE InN film. Recently, some groups reported the observation of strong photoluminescence in InN films with conflicts concerning the exact band gap.[15–22,53,54] These are very significant improvements for InN, because electron concentration below 10^{19}, mobility above $300\,\mathrm{cm^2/V\,s}$, and observation of photoluminescence have never been reported till 1999 in the InN film grown by the most popular growth techniques, MOVPE and MBE. Attempts were also made for the deposition of InN based heterostructures towards the fabrication of InN based electronic devices.[46,55–57] Preliminary evidence of two-dimensional electron gas (2DEG) accumulation in the InN and study on InN-based FET structure were also reported recently.[56,57]

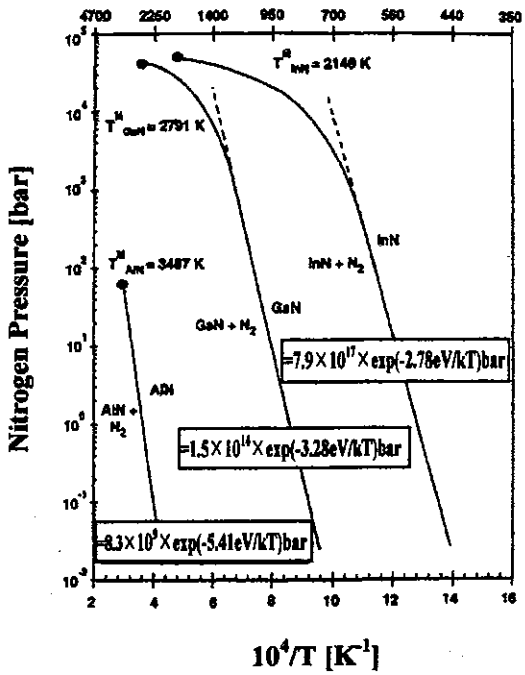

FIG. 2. Melting points of III–nitrides and equilibrium N_2 pressures over the III–N(s) + III(l) system from high pressure experiments and theoretical calculations (Ref. 58).

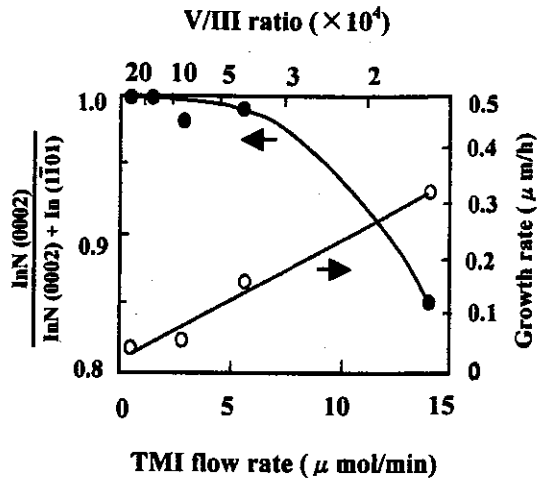

FIG. 3. Relationship between the x-ray peak intensity ratio of InN (0002) to the sum of InN (0002) and metal–indium ($1\bar{1}01$) and the TMI flow rate. V/III ratio and growth rate are also shown (Ref. 60).

II. GROWTH

A. MOVPE

1. Fundamental and influence of basic growth parameters

The growth of InN is the most difficult among the III–nitrides because the equilibrium vapor pressure of nitrogen over the InN is several orders higher than AlN and GaN as shown in the Fig. 2.[58] Because of the low InN dissociation temperature and high equilibrium N_2 vapor pressure over the InN film,[29] the preparation of InN requires a low growth temperature. The source materials generally used for the MOVPE growth of InN are TMI as an In source and ammonia (NH_3) as a nitrogen source. Nitrogen (N_2) is being used as a carrier gas. Due to the low (~500 °C) growth temperature, the MOVPE growth of InN is thought to be restricted by a low decomposition rate of NH_3. Although a higher growth temperature is expected to result in a higher decomposition rate of NH_3, it can also bring about thermal decomposition or thermal etching of the grown InN. On the other hand, growth at a low temperature (lower than 400 °C) is dominated by the formation of metallic In droplets due to the shortage of reactive nitrogen. Epitaxial growth at low temperature becomes impossible due to reduced migration of the deposited materials. Therefore, the region suitable for the deposition of InN is very narrow. Koukitu *et al.* carried out a thermodynamic study on the MOVPE growth of III–nitrides.[59] They pointed out that a high input V/III ratio, the use of an inert carrier gas, and a low mole fraction of the decomposed NH_3 are required for the growth of InN. Experimental results also match well with the first two points (high input V/III ratio and the use of inert carrier gas) but are not clear on the last point (a low mole fraction of the decomposed NH_3). Experimental results show that enhancement of NH_3 decomposition, by increasing growth temperature, V/III ratio and growth pressure, favors the MOVPE growth of InN, as discussed in the following sections. However, the role of NH_3 decomposition or how NH_3 decomposes in the growth atmosphere is not so clear. Matsuoaka *et al.* reported that at a V/III ratio lower than 1.6×10^4, indium droplets formed on a surface.[60] When this ratio was over 8×10^4, the epitaxial layer had a mirror surface. Figure 3 shows the relationship between the x-ray peak intensity ratio of InN (0002) to the sum of InN (0002) and metal–indium ($1\bar{1}01$) and the TMI flow rate. The V/III ratio and growth rate are also shown. The amount of indium droplets present is shown to decrease with increasing the V/III ratio. At a ratio of more than 1.6×10^5, the indium peak in the x-ray diffraction (XRD) spectrum disappears. The object of high input V/III ratio is to provide sufficient amount of reactive nitrogen, since the NH_3 decomposition rate is low at low growth temperature. The above explanations are suited mainly for growth temperatures $\leqq$600 °C. In the case of a relatively high growth temperature (~650 °C) the growth mechanism is different. At such high temperature a high input V/III ratio impedes the growth and a low input V/III is required. It is believed to be that at such temperature the NH_3 decomposition is highly enhanced compared with a low growth temperature ($\leqq$600 °C), and reducing the need for a high input V/III ratio. In addition, enhancement of NH_3 decomposition results in the increase of H_2 partial pressure, which significantly prevents the growth of InN, and therefore, a low input V/III is required. Koukitu *et al.* carried out a detailed thermodynamic study on the role of hydrogen during the MOVPE growth of III–nitrides.[61] They showed that increase of hydrogen in the growth system results in a decrease of the InN deposition rate, which they suggested was due to the decrease of driving force for the deposition. However, at low temperature, the driving force for the deposition is almost independent of the increase of hydrogen partial pressure while at high growth temperature it significantly decreases with increasing hydrogen partial pressure and even reaches a

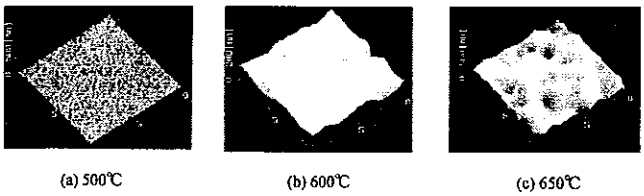

FIG. 4. Surface morphology for the InN film grown on sapphire substrate at a different temperature (Ref. 63).

negative value, which is called etching. Thus the reaction depositing InN proceeds more effectively in the inert gas system and is prevented with the increase of H_2. Therefore it is necessary to use inert carrier gas in the growth of InN or indium containing nitrides while such problems are less significant in the case of GaN or AlN because of their larger equilibrium constant. These theoretical explanations agree with the practical case, as the growth of InN is not possible using a H_2 carrier gas and instead N_2 carrier gas is being widely used for successful growth. Koukitu *et al.* also carried out a thermodynamic analysis on the MOVPE growth of III–nitrides using hydrazine (N_2H_4).[62] They predicted that the growth of nitride occurs rapidly in the N_2H_4 system, especially for the indium containing nitrides, without the deposition of In droplets. It was also shown that effect of hydrogen is small in the N_2H_4 system compared with the NH_3 system. It can be concluded that the temperature region suitable for the deposition of InN using conventional MOVPE system is 400–650 °C. A high input V/III ratio is required for the growth at low temperature while a low input V/III ratio is essential for the high temperature growth. The deposition reaction of InN proceeds more effectively in the inert gas system or N_2 carrier gas and is prevented with increase of H_2 either as a reaction product or as a carrier gas.

The growth temperature in the MOVPE growth of InN is the most critical parameter to control the film quality. Growth temperature significantly influences the crystallinity, surface morphology, growth rate, and electrical properties of the grown InN film. A single crystalline InN film can be grown by MOVPE at a temperature as low as ~400 °C while the upper growth boundary temperature goes as high as ~700 °C. On the basis of the overall quality of the grown InN film, the most suitable region for the MOVPE growth of InN is 500–650 °C. Generally growth at low temperature was found to be columnar due to three-dimensional growth. With increasing the growth temperature, two-dimensional growth is highly enhanced. Figure 4 shows an atomic force microscope image for the InN film grown on α-Al_2O_3(0001) substrate at different temperatures by MOVPE. The MOVPE growth of InN within the temperature 550 °C was found to be columnar while at 600–650 °C continuous film with enhanced two dimensional growth was obtained.[63] For the film grown at ~650 °C, many pits were found to be formed on the enlarged grain surface, most likely due to decomposition or thermal etching of the grown InN film at such high temperature. The crystalline quality measured by x-ray rocking curve (XRC) full width half maximum (FWHM) was also found to be degraded at such high temperature (~650 °C). However, according to Chen *et al.*[64] and Keller *et al.*[55] crystalline quality of the grown InN film degraded even at a temperature lower than 600 °C, which is most likely related to the higher misorientation of the InN grains with increasing the temperature. The growth rate was also found to be dependent on the growth temperature. Figure 5 shows the dependence of the growth rate on the growth temperature for InN film grown in the conventional MOVPE growth mode. The dependence of growth rate on TMI supply is also shown in Fig. 5(b), and also in Fig. 3. The growth rate increases with increasing the growth temperature and TMI supply. Adachi *et al.* carried out a detailed study about the growth rate and its limiting parameters for the MOVPE growth of InN.[65] They showed that the growth rate of InN increases with increasing the temperature at 400–630 °C even at a constant TMI supply, and showed a saturation against an increase in TMI supply, which indicates that the growth rate is limited by NH_3 decomposition at such temperatures. At 630–650 °C, the growth rate is proportional to TMI supply as NH_3 decomposition is highly en-

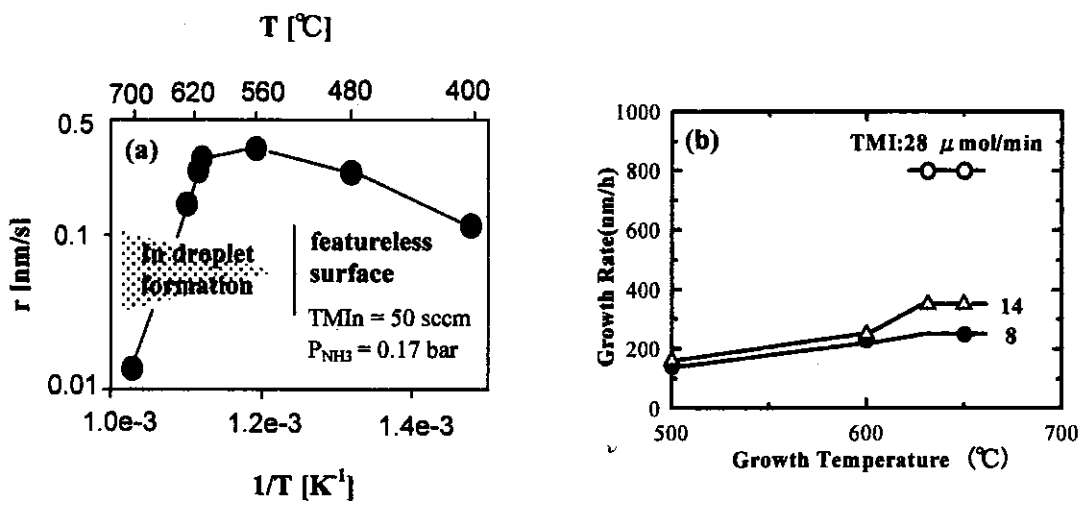

FIG. 5. (a) Dependence of the growth rate on the growth temperature for InN film grown in the conventional MOVPE growth mode (Ref. 55). (b) The growth rate of InN for a different TMI supply as a function growth temperature (Ref. 63).

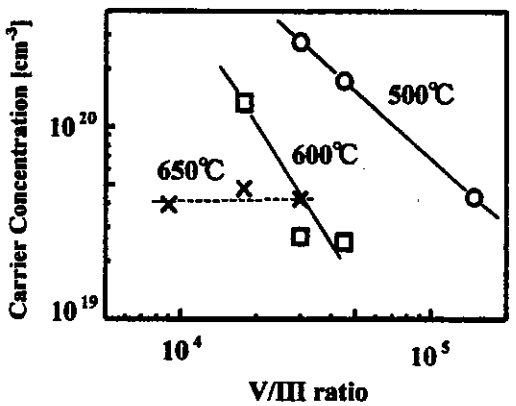

FIG. 6. Carrier concentration of InN grown at a different temperature as a function of V/III. Growth pressure is 0.1 atm (Ref. 63).

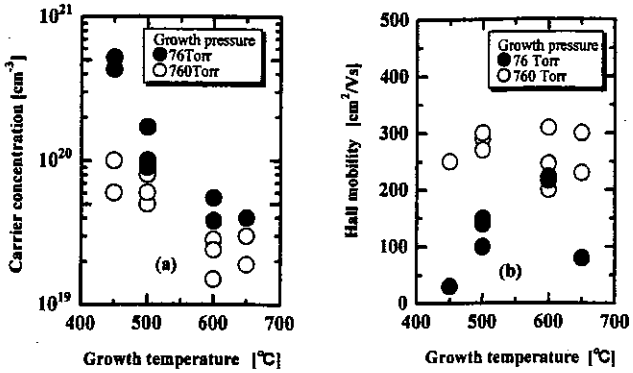

FIG. 7. Growth pressure dependence of (a) carrier concentration and (b) electron mobility for InN film grown at a different temperature (Ref. 63).

hanced and a growth rate as high as 0.8 μm/h was attained at around 650 °C. Above 650 °C, the growth rate decreased with increasing temperature due to decomposition of InN, and In droplet formation dominated. However, according to Keller *et al.* the growth rate drastically decreased with increasing the temperature above 620 °C as shown in Fig. 5(a). The variation of temperature in crystalline quality and growth rate by different groups is likely due to differences in the temperature measurement methods and other parameters of the MOVPE growth system (e.g., horizontal or perpendicular reactor, growth pressure, gas velocity and flow system, susceptor structure, etc.). The growth temperature was also found to be a critical parameter for the electrical properties of the InN films. Keller *et al.* reported that the residual background carrier concentration in the InN film steadily decreased from 2.2×10^{20} to 5.8×10^{18} cm^{-3} when the deposition temperature was increased from 400 to 620 °C, most likely related to a more efficient NH_3 decomposition at higher temperature.[55] Yamamoto *et al.* also reported that the carrier concentration reduces and the Hall mobility increases with increasing the growth temperature.[63] It was also found that increase in the NH_3/TMI molar ratio reduces the background carrier concentration within a growth temperature of 600 °C. Figure 6 shows the carrier concentration of InN grown at different temperatures as a function of V/III. These results suggest that the increase in temperature and V/III ratio brings about a reduction of nitrogen vacancies in the InN by increasing active nitrogen in the growth atmosphere. Thus, the growth reaction for MOVPE InN at around 600 °C is dominated by the nitrogen supply, and the shortage of active nitrogen during the growth (i.e., nitrogen vacancy) seems to be responsible for the high background donor concentration in the InN film. However, the carrier concentration was found to be independent on the V/III ratio in the InN film grown at a temperature around 650 °C, as shown in the Fig. 6. This fact suggests that another mechanism governs the electrical properties for the InN film grown at around 650 °C, most likely thermal decomposition. From the experimental as well as theoretical basis, the most suitable region for the MOVPE growth of InN is 550–650 °C. In the case of MBE, the suitable temperature region is a little lower than MOVPE.

Growth pressure is also one of the basic parameters in the MOVPE growth system. There is no detailed investigation about the influence of growth pressure in the MOVPE growth of InN. In the conventional MOVPE growth of InN, either atmospheric-pressure (760 Torr) or low-pressure (76 Torr) growth has been generally performed. However, differences resulting from varying the growth pressure was not studied in detail.[13,63,66] It was found that growth pressure significantly influences the grown InN film, especially electrical properties. At low growth temperature (~450 °C) the crystalline quality of the InN film grown in a low pressure was found to be better than the film grown in an atmospheric pressure.[13] However, the electrical properties of the InN film grown in an atmospheric pressure was found to be better than the film grown in a low pressure, over the entire temperature range,[63,66] as shown in Fig. 7. This is because the atmospheric pressure growth is one of the means to enhance the NH_3 decomposition as a result of reduced flow velocity of the reactant gases. It also can suppress nitrogen evaporation during the growth. Therefore, atmospheric pressure growth can provide more reactive nitrogen as well as can suppress the nitrogen evaporation from the grown InN, which reduces the nitrogen vacancy and gives better electrical properties. By employing an atmospheric growth, a MOVPE InN film with a carrier concentration in the order of 10^{18} cm^{-3} was successfully grown with high electron mobility (~700 cm^2/V s).[67] The lowest carrier concentration and highest mobility in the InN film grown in a low pressure were found to be 4×10^{19} cm^{-3} and ~300 cm^2/V s respectively.[63]

In the MOVPE growth of III–nitrides reactor design has also been found to be an important factor to obtain high quality grown film. For example, Nakamura *et al.* reported that high quality GaN film could be grown using a two-flow MOVPE reactor, where an inactive sub flow gas was used to change the direction of the reactant gas in contact with the substrate surface.[68] Nishida *et al.* have improved the GaN film quality by employing a MOVPE horizontal reactor with separate carrier gas and reactant gas entry, in which the carrier gas in the upper stream suppresses the reactant gas to form a laminar flow pattern above the susceptor.[69] Yang *et al.* studied the effect of reactant gas flow spacing between the substrate and the ceiling of the quartz chamber on the

morphology of the grown GaN film, and discussed their results with the boundary-layer model.[70] Yamamoto *et al.* studied the influence of reactor design on the MOVPE growth of InN and found that reactor design significantly influences the grown InN film.[71] They studied the MOVPE growth of InN using two different designs of horizontal reactor. The major difference between the two designs is a variation in the reactant gas flow spacing between the substrate and the ceiling of the quartz chamber, which results variation in the speed of reactant gas flow. It was found that the reactor with a high speed gas flow brings about InN film with a large grain size, and when InN film is grown at 600 °C two-dimensional (2D) growth was found to be extremely enhanced. The enhanced 2D growth results in a smaller XRC-FWHM. The primary cause was concluded to be a decrease in the effective NH_3/TMIn ratio in the growth atmosphere. Yang *et al.* studied the effect of reactant gas velocity on the MOVPE growth of InN.[72] With a high-speed reactant gas, the thickness of the stagnant layer is reduced so that the reactant species can reach the surface effectively. A layer-like growth of InN was achieved, resulting in a marked improvement of the film quality. In addition, significant enhancement of the growth rate up to 2 μm/h was obtained.

Flow modulation epitaxy attracted interest and has been investigated as well to obtain high quality III–nitride grown films. In this technique, the group V and III species are injected alternately or one is pulsed for a different time period while the other is kept constant during the growth. High quality GaN film has been grown by this technique.[73] Keller *et al.* studied the flow modulation epitaxy of InN on semi-insulating GaN on *c*-plane sapphire substrate by applying modulated precursor injection schemes, where (a) the NH_3 flow was kept constant, but the TMI was pulsed for a different time period (injected for 12 s followed by a 9.5 s long flow interruption), and (b) TMI and NH_3 were injected alternately.[55] It was found that the modulated precursor injection schemes were effective in suppressing the grain growth and also In droplet formation at higher InN growth temperature. When TMI and NH_3 were injected alternately, in an atomic layer epitaxy (ALE) like growth mode following procedure, surface steps were clearly visible. Grain formation was also prevented, when TMI was injected in a pulsed manner. The alternate injection procedure drastically suppressed also the formation of metal droplets on the surface, where as droplets were still found on the surfaces of film grown using pulsed TMI injection, due to the simultaneous presence of both TMI and NH_3 in the gas phase. However, the overall growth rate was lower than the conventional growth mode, possibly related to desorption of species from the surface in the "zero-growth" phase of the injection cycle. The carrier concentration in the layer increased with decreasing growth rate and flush/growth interruption time in the cycle. Thus, for the thin InN layer grown using both procedure (a) and (b) free carrier concentrations of $\sim 10^{20}$ cm^{-3} were reported.

2. Modified MOVPE system

Plasma-assisted MOVPE employs reactive nitrogen radicals produced by plasma dissociation, which is independent of the growth temperature. Single crystalline epitaxial InN films reported by Wakahara *et al.* were grown by using plasma-assisted MOVPE.[49,50] Many research works have been carried out using plasma-assisted MOVPE in a wide range of growth condition and on different substrates.[74–85] There were very few reports about the electrical properties,[50,81] and growth of high quality InN by using plasma-assisted MOVPE has not been reported yet, which is now the focus of InN research. Compared to the conventional MOVPE and MBE, the InN films grown by plasma-assisted MOVPE are inferior and reported data are insufficient. Much of the good quality InN films grown today are produced using conventional MOVPE by reacting TMI with NH_3 at a different substrate temperature, as well as by MBE.

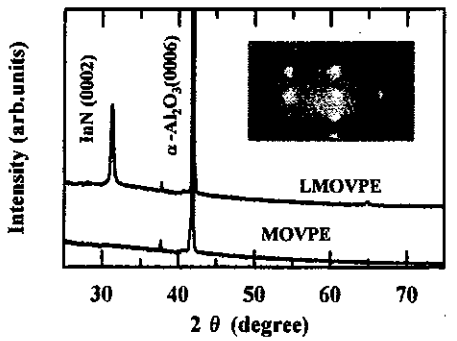

FIG. 8. XRD spectra from the InN grown on sapphire at 350 °C by LMOVPE and conventional MOVPE (without laser). The inset is the RHEED pattern of the InN grown by LMOVPE (Ref. 87).

Laser-assisted MOVPE is a potential growth technique, which can provide reactive N and In radicals by photolysis of their precursors independent of the growth temperature. In this technique an ArF excimer laser is used which can photolytically dissociate NH_3, and organic precursors [TMI, triethylindium, etc.], and therefore, the film can be grown at a low temperature. It is also thought to be advantageous in reducing the nitrogen vacancies in InN film due to the temperature independence of the partial pressure of nitrogen over the InN film. Li *et al.* studied the laser assisted (LA)-MOVPE growth of III–nitrides but the InN film grown was not stoichiometric.[86] Recently, Bhuiyan *et al.* successfully obtained single crystalline InN film on sapphire substrate by LA-MOVPE at a temperature as low as ~350 °C while thermal growth at such low temperature (i.e., without laser) was not possible, as shown in Fig. 8.[87] In addition to that the LA-MOVPE was found to be a potential technique to obtain selective area growth of InN by varying the laser beam pattern incident on the substrate. Recently, significant progress in the epitaxial growth of InN by the LA-MOVPE has been obtained. Single crystalline InN film with high growth rate and smooth surface has been obtained over a wide range of temperature and condition just by flowing a small amount of total reactant gases.[88]

B. MBE

1. Source materials and growth kinetics

In the MBE growth of III–nitrides, the solid sources of the group III elements such as Ga, In, and Al are used in

general, but the nitrogen is supplied by the gas source such as N_2 and NH_3. In general, this type of MBE system is called gas source MBE.[89] The metalorganic chemical beams are also sometimes used as the group III element sources and then it is called metalorganic molecular beam epitaxy (MOMBE) or chemical beam epitaxy.[90] In both types of MBE, the key issue in the growth is the nitrogen source. The dissociation energy of N_2 molecules is as high as 9.5 eV, therefore, the supply of N_2 gas to the substrate surface with the group-III elemental beams can not induce any growth of the nitrides. For obtaining atomic reactive nitrogen, the N_2 molecules are dissociated by the radio-frequency (rf)-plasma or the electron cyclotron resonance (ECR) method. Although the rf-plasma source is the most popular and the rf-radical source produces considerably fewer ions than an ECR source due to the higher plasma pressures,[91] it is well known that ion damage can still induce during the epitaxy.[92] Some techniques to avoid such ion damage by an ion tapping system using the static electric field have been tried.[93–95] The other serious problems induced by the plasma may be some contamination such as oxygen or carbon dioxide. To minimize this the discharge may be electrodeless and the plasma contained in a pyrolytic boron nitride (PBN) discharge tube capped with a PBN exit plate.[96] The generation rate of the reactive atomic nitrogen strongly depends on the aperture size and density, the small aperture size and the high aperture density prefer to obtain the high generation rate of reactive atomic nitrogen with less nitrogen ions generation. In ECR plasma source, the generation rate of nitrogen ion increases with increasing the input microwave power. It is well known that the nitrogen ions with energy higher than ~60 eV induce defects in the epitaxial layer. In the case of ammonia (NH_3) or dimethylhydragen (DMHy) gases, they are supplied to the substrate surface without any cracking, because the cracking promotes the N_2 molecular generation.[97–102] It is not so clear about the catalytic effect in the dissociation process of the NH_3 or DMHy on the In surface, although the catalytic effect of those can be observed on the Ga or Al surfaces above 700 °C[97–101] or 600 °C,[102] respectively.

Koukitu and Seki have reported a thermodynamic analysis on the MBE growth of III–nitrides.[103] The equilibrium partial pressure and the growth rate were calculated for input V/III ratio, input partial pressure of group III elements and growth temperature. A summary of their calculation results as a phase diagram for the deposition, indicating etching, droplet and growth regions are shown in the Fig. 9. The chemical reaction, which connects all species at the substrate surface, is

$$\mathrm{In}(g)+\mathrm{N}(g)=\mathrm{InN}(s). \tag{1}$$

The equilibrium equation for the reaction is as follows:

$$K1=1/(P_{\mathrm{In}}+P_{\mathrm{N}}). \tag{2}$$

From the conservation constraint we have

$$P^0_{\mathrm{In}}-P_{\mathrm{In}}=P^0_{\mathrm{N}}-P_{\mathrm{N}}, \tag{3}$$

where P^0_{In} and P^0_{N} are the input partial pressures, which are obtained from the incident beam flux, and P_{In} and P_{N} are the equilibrium partial pressures. Equation (3) expresses that the

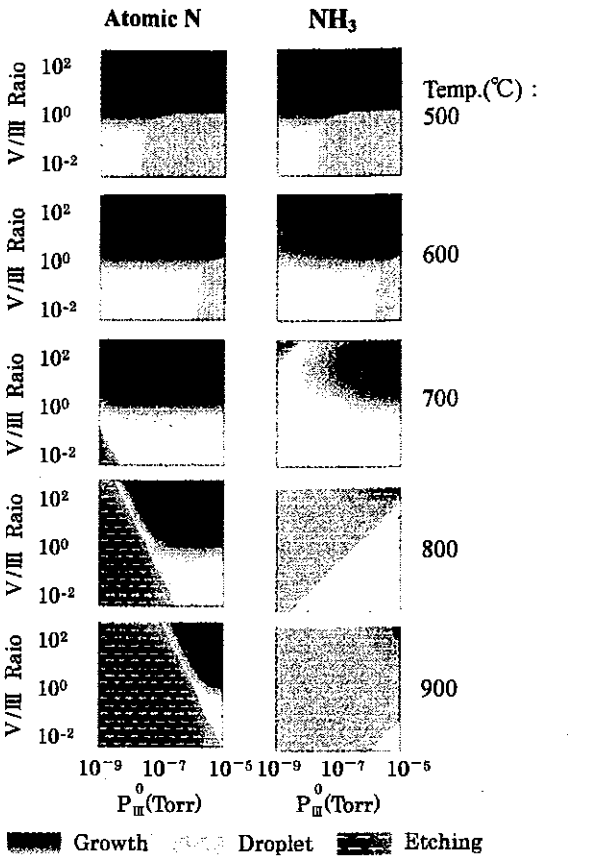

FIG. 9. The calculated phase diagram for the MBE deposition of InN using atomic N and NH_3 gases. There are three deposition modes: etching, droplet and growth (Ref. 103).

deposition occurs in the ratio of 1:1 for In and N. The equilibrium partial pressures at the substrate surface can be obtained from the solution of the above simultaneous equations. The value of the equilibrium constant was obtained from the literature.[103] The corresponding free energy to the chemical reaction (1) used in the analysis is as follows:

$$\Delta G^0(\mathrm{kcal/mol})=(-1.764\times10^2)+3.067\times10^2/T+(-1.451\times10^{-3})\times T\times\ln(T)+7.909\times10^{-2}\times T+3.883\times10^{-11}\times T\times T. \tag{4}$$

The calculation for the MBE system using an NH_3 source was performed in a similar manner, using atomic nitrogen. The chemical reaction is

$$\mathrm{In}(g)+\mathrm{NH_3}(g)=\mathrm{InN}(s)+(3/2)\mathrm{H_2}(g). \tag{5}$$

In NH_3 case, they introduce α, the molar fraction of decomposed NH_3, into the calculation as follows:

$$\mathrm{NH_3}(g)\Rightarrow(1-\alpha)\mathrm{NH_3}(g)+(\alpha/2)\mathrm{N_2}(g)+(3\alpha/2)\mathrm{H_2}(g). \tag{6}$$

The value of α is assumed appropriately as that of MOVPE growth,[104] because it is difficult to know the exact value. The equilibrium partial pressure and the growth rate were calculated for input V/III ratio, input partial pressure of In, and growth temperature. In the growth of InN, they conclude that three deposition modes, i.e., etching, droplet and growth re-

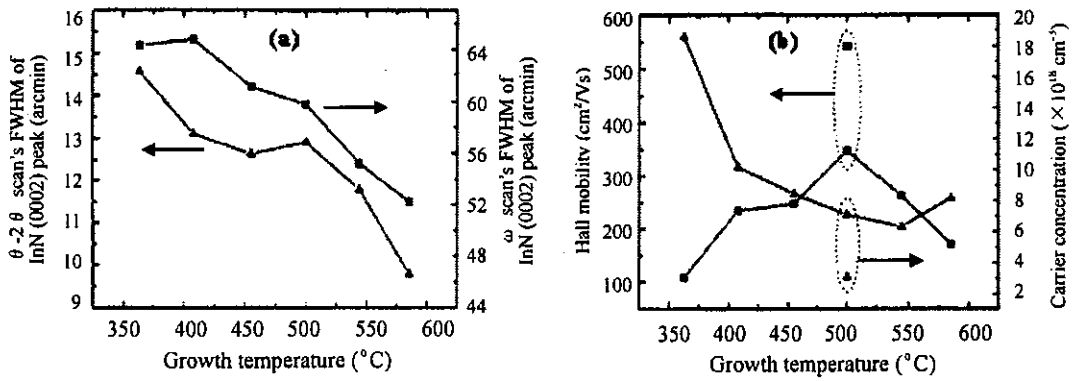

FIG. 10. The growth temperature dependence of (a) FWHM of the InN (0002) peak and (b) the electrical properties of the InN film grown by MEE (Ref. 108).

gions, appear in the temperature range from 500 to 900 °C. The growth temperature suitable for the InN growth is predicted to be from 600 to 700 °C with V/III≥1, which is essential in the MBE growth. However, the experimental growth temperature is much lower than this theoretical prediction, and almost experiments have been done in the temperature range from 450 to 550 °C. They also reported that there is a difference between the atomic nitrogen and the NH_3 source as shown in the corner of diagram (Fig. 9) where the etching region appears. In the case of the atomic nitrogen source, the etching region appears constantly at the region where the input V/III ratio and the input P^0_{In} are low value. On the other hand, in the case of the NH_3 source, it appears at the region where the V/III ratio is high and the input P^0_{In} is low value. They have pointed out that this is due to the decomposition of NH_3: when NH_3 is decomposed, H_2 gas is produced, and the produced H_2 drives Eq. (5) to the left hand. Consequently, the deposition moves into the etching mode due to the increase in H_2.

2. Growth mode and influence of basic growth parameters

The growth mode problem is an interesting one to improve the film quality in the InN lattice-mismatched heteroepitaxy. The 2D growth mode is preferable. Ng *et al.* investigated the relationship between the film growth mode and the deposition conditions in the plasma-assisted molecular beam epitaxy of the InN on GaN (0001) templates.[105] Surprisingly, they have observed both 2D and 3D [Stransky–Krastanov (SK)] growth modes in spite of the about 10% lattice mismatch, and the growth mode is seen to be controlled by growth condition: low temperature or high N flux (relative to In) favors SK growth, whereas high temperature and high In flux leads to 2D growth. They also reported that strain in the InN begins to relax upon the first layer deposition and almost completes after 2–4 bilayers growth and the 3D islands form after most of the strain has been relieved for the case of SK growth, therefore, the islands are likely dislocated and strain free. Norenberg *et al.* investigated the MBE growth of InN on GaN/Al_2O_3 (0001) and Si (111) substrates using NH_3 instead of nitrogen plasma for the supply of the group-V atoms.[106] They also observed the growth of 2D InN islands on the GaN template substrate and that only a pre-exposition of the GaN substrate to silicon enables a growth mode change from 2D to 3D. Later on, they studied the growth of self-assembled InN nanostructures on GaN by MBE using both cracked NH_3 and a nitrogen plasma as the group V source.[107] They pointed out that Stranski–Krastanov growth may be achieved but is highly sensitive to the V/III ratio as well as coverage and temperature. The size and shape of the resultant nanostructure depend on the nitrogen source used.

Growth temperature is one of the most important growth parameters. In MBE growth, most experiments have been done in the temperature range from 450 to 550 °C. In the two-step growth, however, the low temperature buffer layer is grown at temperatures ≤350 °C. Usually, the annealing temperature after the low-temperature buffer layer growth is often same temperature range of the epitaxial growth. Above the epitaxial growth temperature range, the growth rate of the InN becomes extremely low or the InN growth does not occur because of InN dissociation and the re-evaporation of In from the surface. Below the epitaxial growth temperature range, such as the temperature for the buffer layer growth, the crystal quality of the layers is usually quite bad. Annealing brings a significant improvement in the grown film quality. The growth temperature dependence of the FWHM of the InN (0002) peak and the electrical properties studied in the InN film grown by migration enhanced epitaxy (MEE) is shown in Fig. 10.[108] This implies that the crystalline quality improves with increasing the growth temperature. The electrical properties also improve with raising the temperature from 350 to 500 °C, and then deteriorates as the temperature is further raised. Recently, Saito *et al.* also confirmed that the crystalline quality of the rf-MBE grown InN was improved by increasing the growth temperature within the dissociation limit of InN.[109] They also reported that the growth temperature significantly influences the epitaxial relationship and polarity of the grown InN film.[110,111] The dominant factor in determining the main epitaxial relationship is growth temperature and the polarity of InN is much more sensitive to growth temperature compared with other nitride semiconductors. Xu *et al.* have investigated the effects of substrate temperature and surface stoichiometry on the growth behavior of rf-MBE InN.[112] They found that N-rich conditions are favorable for stable InN growth at growth temperatures rang-

ing from 470 to 590 °C. They also showed that under the In-limited growth condition, the step flow growth was achieved on N-polarity GaN template at 580 °C with a growth rate of 1.3 μm/h.

C. MOMBE

MOMBE is also one of the potential growth techniques where the advantages of both MOVPE and MBE can be utilized. Film can be grown relatively at low temperature by MOMBE and premature reaction of the precursors, a serious problem in MOVPE, is minimized due to the large mean free path of gaseous molecules. Compared with MBE technique, MOMBE has several advantages, such as, no downtime for source replacement and has the potential for scale-up. In spite of the variety of heteroepitaxial growth techniques of InN, few have been reported for MOMBE. Abernathy *et al.* demonstrated the growth of InN by MOMBE using TMI and ECR generated nitrogen plasma.[113] The grown InN film was fine-grained polycrystalline, and they evaluated the resitivity, growth rate, electrical properties, and surface morphology as a function of microwave power, growth temperature and trimethylindium flux. They showed that the growth rate declines with increasing the temperature from 400 °C, suggesting that the TMI desorption rate is increasing with temperature. The morphology was generally independent of growth temperature and the electrical properties improve with temperature. The film characteristic was also evaluated as a function of TMI flow for a fixed nitrogen flow and plasma power. They showed that the growth rate increases with TMI flow, and the electrical properties improve with TMI flow in the initial stage. However, in their study the carrier concentration was high ($>10^{20}$ cm^{-3}) and mobility was low (~ 100 cm^2/V s). Recently, Aderhold *et al.* have successfully grown InN on sapphire substrate by MOMBE.[114] They explained that the quality of InN epilayer could be improved by an appropriate choice of nucleation layer and growth condition. Using a GaN nucleation layer good quality InN thin film was obtained on the sapphire substrate with a carrier concentration as low as 8.8 $\times 10^{18}$ cm^{-3} and a mobility of 500 cm^2/V s at room temperature. Further growth process optimization should prove the MOMBE technique as an excellent candidate for high quality InN thin film production.

D. Sputtering

Sputtering was the most widely studied and the earliest successful growth technique for InN.[12,14,30,32,37–46,115–136] It is a relatively inexpensive and simple growth approach, and film can be grown at low temperature. Nataranjan *et al.* demonstrated the detail mechanism of reactive sputtering of indium, and growth of InN in mixed Ar–N_2 discharges.[37] Part of the success of rf-sputtering was thought due to the low growth temperature that may be accessed—this is important since severe nitrogen loss from InN occurs at temperature above 550 °C.[135] Unfortunately, the InN film prepared by reactive sputtering in other laboratories has not met these expectations. The previous sputtering growth technique has been upgraded and even single crystalline epitaxial film of InN has been grown. However, the film qualities are very poor and have universally high carrier concentration near 10^{20} cm^{-3} and constantly low electron mobility of less than 100 cm^2/V s. Even the original reactive sputtering unit of Tansley and Foley is still in existence and has been substantially upgraded but is being unable to reproduce the same InN film with the best reported data.[135]

E. HVPE

The first epitaxial growth of InN was demonstrated by HVPE.[36] Recently, HVPE has received much attention because of its high growth rate compared with that of MOVPE and MBE. The HVPE process is a chemical vapor deposition method, which is usually carried out in a hot wall reactor (horizontal or vertical) at atmospheric pressure. The source materials generally used for the HVPE growth of InN are indium monochloride (InCl) or indium trichloride ($InCl_3$) as In source, and ammonia (NH_3) or monomethylhydrazine (MMHy) as N source. The InCl is usually synthesized in the upstream of the reactor by reacting HCl gas with metallic In and the $InCl_3$ is presynthesized. Because of the group III element is transported to the substrate as a volatile compound (usually a chloride), this technique is often referred to as chloride-transport vapor phase epitaxy (VPE).

Marasina *et al.* studied the HVPE growth of InN using the interaction of $InCl_3$ and NH_3, and discussed the growth kinetics of InN epitaxial layer.[36] Their experimental data proved the correlation between the $InCl_3$ vapor concentration and the structure perfection of InN epitaxial layer at the constant temperature in the deposition zone. They found the optimum temperature range for $InCl_3$ evaporation is 450–520 °C, and an increase of the temperature from 450 to 600 °C (the corresponding $InCl_3$ concentration increased from 4 to 12 mg/l) resulted in the increase of the growth rate from 1 to 8 μm/h at a constant substrate temperature (T_s = 630 °C). Igarashi clearly showed the single crystalline growth of InN using vapor phase reaction of In–Br_2–N_2–NH_3 system, where mixture of N_2 and Br_2 was passed over the heated In to transport the volatile indium bromides to the deposition zone.[137] Sato and Sato studied the HVPE growth of InN using the monochloride of group III element and hydride of the group V element (InCl and NH_3, respectively).[138] They obtained InN film over the range of growth temperature from 455 to 510 °C and of the V/III supply ratio from 500 to 2000. The electrical properties were poor and found to be deteriorated with decreasing the NH_3 gas flow rate. Takahashi *et al.* carried out some significant works on the HVPE growth of InN.[139,140] Figure 11 shows the growth rate of InN as a function of V/III ratio for several source combinations. As seen in the Fig. 11, no growth was observed with the $InCl_3$–MMHy system while some growth was observed with the InCl–NH_3 and InCl–MMHy systems. In contrast with these systems, an appreciable growth was observed with the $InCl_3$–NH_3 system. They showed that the growth rate initially increases with increasing the growth temperature up to 550 °C and then gradually decreases to 700 °C. They found that the growth rate decreases with increasing H_2 molar fraction in the carrier gas and the growth

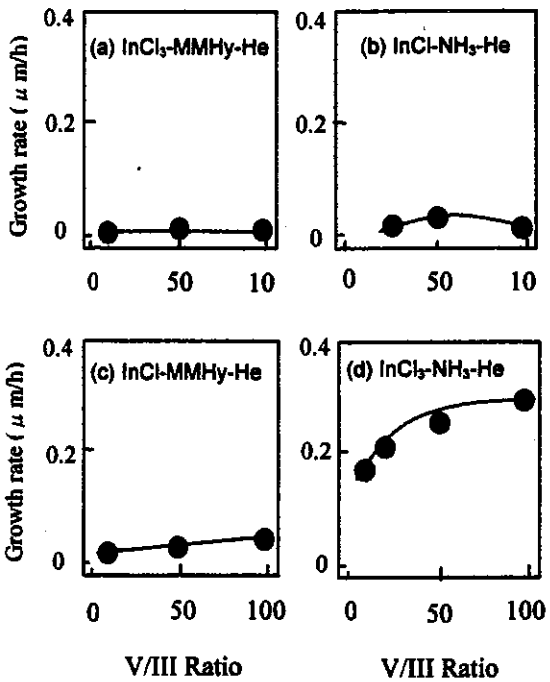

FIG. 11. The HVPE growth rate of InN as a function of V/III ratio for several combination of sources at a growth temperature of 500 °C (Ref. 139).

ceases when the H_2 molar fraction increases up to about 10%, therefore, growth in an inert gas is indispensable. This is supported by the work of Sunakawa *et al.*, in that use of inert carrier gas, such as nitrogen, was crucial for the growth and almost no growth was observed when H_2 carrier gas was used.[141] In both the reports, use of indium trichloride ($InCl_3$) as In source was emphasized. In the conventional VPE growth, such as GaAs and InP, monochlorides are used as group III sources. However, trichloride ($InCl_3$) reacts more effectively than monochloride (InCl) in the InN growth. This may be ascribed to the fact that the formation of an adduct ($InCl_3.NH_3$) between $InCl_3$ and NH_3 occurs easily in the $InCl_3-NH_3$ system. Takahashi *et al.* also obtained hexagonal InN epitaxial layer reproducibly at a growth temperature as high as 750 °C,[140] and found that a high input partial pressure of $InCl_3$ was necessary for the growth of InN at high temperature.

F. Pulsed laser deposition (PLD)

The PLD technique has also been investigated to grow high quality III–nitride films.[142,143] This is a vacuum based process where film is deposited on the substrate by laser ablation of the solid nitride or metal target. Since the average energy of the laser-ablated species is considerably higher ($100-200\,kT$) than the thermal energy kT, it is possible to lower the growth temperature of the film. Feiler *et al.* were the first to deposit InN film on sapphire substrate by PLD.[144] The grown film was not single crystal, but instead was found to have a preferred orientation with InN(0001)// sapphire(0001) and InN[$1\bar{1}00$]//sapphire[$10\bar{1}0$]. The InN films grown in high vacuum and 5 mTorr of N_2 were both p type with carrier concentration of 6.5×10^{20} and 4.7 $\times10^{19}$ cm^{-3} and mobility of 30 and 240 $cm^2/V\,s$, respectively. In addition, both films were found to have indium droplets present on their surfaces. This is the only report of p-type InN, which to date has never been observed for unintentionally doped InN film grown by other methods. Recently, Bhattacharya *et al.* reported the InN growth by N_2 glow discharge plasma-assisted pulsed laser deposition using elemental In as a target.[145] The InN film was grown on sapphire substrate at 400 °C, and was found to have predominant zincblende (ZB) structure along with a low-intensity hexagonal wurtzite (WZ). They measured the band gap of the grown InN film from optical absorption spectra and was found to be about 1.9 eV.

G. Other methods of InN growth

Other methods used include reactive evaporation,[31,47,146,147] electron beam plasma techniques,[33,34] growth of InN by low energy modulated indium and nitrogen beams,[148] solvo-thermal method,[149] etc. Among these growth techniques, reactive evaporation is a simple method and widely studied. In the early days, Trainor and Rose grew InN on sapphire by reactive evaporation method and reported some properties (optical and electrical) of grown InN film.[31] Sato and Sato carried out some important works on the growth of InN by reactive evaporation. They reported that the carrier concentration of the InN film shows a significant decrease, from 3.2×10^{20} to 4.3×10^{18} cm^{-3}, by lowering the growth rate from 0.23 to 0.05 μm/h.[147] Among the other growth techniques, the solvo-thermal method is a notable one and recently reported technique.[149] Using this method, indium nitride (InN) nanocrystals were successfully prepared by the reaction of $InCl_3$ and Li_3N at 250 °C with xylene as the solvent. The particles had good dispersion with the average size of 28 nm.

III. SUBSTRATES AND BUFFER LAYERS

A. Substrates

1. Sapphire

Sapphire is the most extensively used substrate material for the epitaxial growth of InN. Large area good quality crystals of sapphire are easily available at relatively low cost. They are transparent and stable at high temperature. High quality epitaxial InN film can be grown easily on sapphire substrates by the popular growth methods, MOVPE and MBE. The band gap and lattice constant in the hexagonal atomic space-plane of InN and the materials which are widely used as a substrate or underlying layer for the epitaxial growth of InN are shown in the Fig. 12. The InN has a large lattice mismatch of ~25% with sapphire compared with the other substrates. The large lattice mismatch and thermal expansion coefficient difference can result in an extremely high density of structural defects. However, researchers have revealed that the substrate surface pretreatment and insert in of an intermediate buffer layer between the substrate and epilayer can significantly improve the film quality. Nitridation of the sapphire substrate surface significantly improves the crystalline quality of InN as a result of

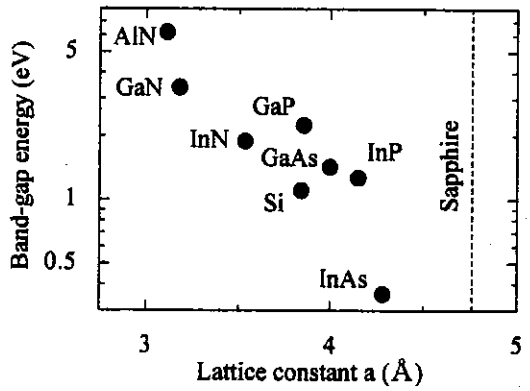

FIG. 12. Band gap and lattice constant in the hexagonal atomic space plane of InN and the materials which are widely used as a substrate or underlying layer for the epitaxial growth of InN.

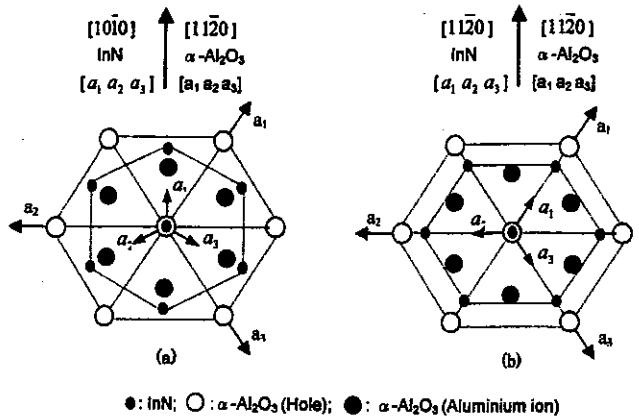

FIG. 13. Schematic illustration of the relation in crystallographic orientation between the (0001) InN film and (0001) α-Al_2O_3 substrate: (a) $[10\bar{1}0]_{InN}//[11\bar{2}0]_{Al_2O_3}$; (b) $[11\bar{2}0]_{InN}//[11\bar{2}0]_{Al_2O_3}$ (Ref. 77).

the formation of AlN.[150–152] The marked improvement of InN film quality by the formation of an AlN layer is due to the fact that AlN has the same lattice structure as InN, and the lattice mismatch is reduced from ~25% for InN/α-Al_2O_3 to 13% for InN/AlN.[150] The quality of the InN film is strongly influenced by the nitridation condition, temperature and time.[151,152] In addition to the substrate surface treatment it was found that incorporation of a buffer layer of AlN, GaN or InN greatly improves the structural and electrical properties of the InN films grown on sapphire substrate.

Generally the epitaxial InN film grown on sapphire is found to be hexagonal wurtzite. However, there are few reports about the formation of cubic structure also. Chen *et al.* reported the formation of mixed hexagonal and cubic structures at low growth temperature between 375 and 450 °C.[153] The crystal orientation of sapphire and InN (grown on *c*-plane [0001] sapphire) is parallel. However, there are different reports about the epitaxial relationship of the *a* axis between InN films and sapphire substrate. When the InN film is grown on nitrided sapphire substrate (or on sapphire using an AlN or GaN layer), the epitaxial relationship between InN, AlN, and α-Al_2O_3 was found to be $[10\bar{1}0]_{InN}//[10\bar{1}0]_{AlN}//[11\bar{2}0]_{Al_2O_3}$. This means that the unit cell of InN and AlN (formed as a results of nitridation or grown AlN or GaN layer) is rotated by 30° about the *c* axis with respect to the sapphire unit cell. This is because the lattice mismatch in the $[10\bar{1}0]_{AlN\text{ or }GaN}//[11\bar{2}0]_{Al_2O_3}$ orientation is much smaller than $[11\bar{2}0]_{AlN\text{ or }GaN}//[11\bar{2}0]_{Al_2O_3}$ orientation, and obviously the epitaxial layer of AlN or GaN is grown more easily in the $[10\bar{1}0]_{AlN\text{ or }GaN}//[11\bar{2}0]_{Al_2O_3}$ orientation, which results the same orientation in InN film. However, when the InN film is grown directly on α-Al_2O_3 (without nitridaton) it can have both the epitaxial relationships of $[10\bar{1}0]_{InN}//[11\bar{2}0]_{Al_2O_3}$ and $[11\bar{2}0]_{InN}//[11\bar{2}0]_{Al_2O_3}$ or any one of them depending on the growth technique or condition. This is because the lattice mismatches of InN are relatively closed in both the two arrangements while those of AlN and GaN differ significantly. The schematic representation of in-plane atomic arrangement of (0001) InN film and (0001) α-Al_2O_3 substrate in both the epitaxial relationships of $[10\bar{1}0]_{InN}//[11\bar{2}0]_{Al_2O_3}$ and $[11\bar{2}0]_{InN}//[11\bar{2}0]_{Al_2O_3}$ is shown in Fig. 13. Guo *et al.* carried out a comprehensive investigation of the structural properties of ME-MOVPE grown InN film and showed the epitaxial relationship of InN film grown directly on α-Al_2O_3 substrate to be $[10\bar{1}0]_{InN}//[10\bar{1}0]_{\alpha\text{-}Al_2O_3}$.[77] However, Yamaguchi *et al.* reported that the InN film directly grown on sapphire substrate by rf-MBE has a tendency to form a multidomain structure due to in-plane rotation, and can have both the epitaxial relationships of $[10\bar{1}0]_{InN}//[11\bar{2}0]_{Al_2O_3}$ and $[11\bar{2}0]_{InN}//[11\bar{2}0]_{Al_2O_3}$ as well as a domain with $[14\bar{5}0]_{InN}//[11\bar{2}0]_{Al_2O_3}$ (rotated by 19° from the substrate).[110] The domain with $[11\bar{2}0]_{InN}//[11\bar{2}0]_{Al_2O_3}$ is mainly observed at relatively low growth temperature of around 520 °C while the domain with $[10\bar{1}0]_{InN}//[11\bar{2}0]_{Al_2O_3}$ becomes dominant with increasing growth temperature to around 540 °C. Therefore, they concluded that the dominant factor in determining the main epitaxial relationship is its growth temperature.

2. Si substrate

Si is a suitable semiconductor substrate material for InN having smaller lattice mismatch compared with the commonly used insulating sapphire substrate; 8% for InN(0001)/Si(111) and 25% for InN(0001)/α-Al_2O_3(0001). In the early days of InN growth, Si was widely used as a substrate but the film quality was very poor. Yamamoto *et al.* attempted the MOVPE growth of InN on Si substrate for the first time in 1994.[13,150] The MOVPE growth of InN directly on Si substrate was unsuccessful because of the formation of an amorphous SiN_x layer on the substrate surface, as a result of the unintentional nitridation of the substrate surface during the growth. The Si substrate surface becomes nitrided during the growth even at a low growth temperature (~400 °C), which forms SiN_x on the substrate surface and caused poor effect on the grown InN film. On the other hand, growth at a temperature lower than 400 °C was found to be polycrystalline due to reduced migration of the deposited

materials on Si and/or reduced decomposition rate of the raw materials. Later, a GaAs intermediate layer on Si substrate was used to avoid the surface nitridation and the InN film was successfully grown on Si substrate using a GaAs(111) intermediate layer.[154,155] Recently, Yodo *et al.* have reported the growth of InN film on Si substrate by ECR MBE.[53,54] They claimed to have obtained InN layer on Si (111) and Si (001), which exhibited strong band edge PL emission at room temperature. They demonstrated by XRD analysis that the InN film exhibited the dominant hexagonal WZ structure along with a low-intensity ZB.

3. GaAs and InAs

The lattice mismatch between InN and GaAs is about 11.5%, which is smaller than that for sapphire, which is about 25%. Sato and Sato reported the epitaxial growth of InN on GaAs substrate by a rf excited reactive evaporation method in 1989.[47] They used GaAs(111)*A* and GaAs(100) as a substrate and reported that the InN film grown on GaAs(111) was found to be single crystalline with an epitaxial relationship of InN(0001)//GaAs(111) while the film grown on the GaAs(100) was weakly oriented polycrystalline. In 1993, Abernathy *et al.* studied the deposition of the InN film on GaAs by ECR-MOMBE but the film was polycrystalline.[113] Strite *et al.* reported the observation of the zincblende polytype of the InN on GaAs(100) substrate by plasma enhanced molecular beam epitaxy.[156] Single crystalline growth of InN on GaAs(111) using microwave-excited MOVPE was reported by Guo *et al.* in 1995.[78] They reported that the pretreatment of the substrate, i.e., exposing the substrate to nitrogen plasma before the growth, is essential for obtaining the epitaxial layer of InN on GaAs(111), and that the crystalline quality of the InN film is strongly dependent on the exposing time.[78] The same group also reported the low temperature (~100 °C) growth of InN on GaAs(111) substrate by radio frequency magnetron sputtering in 1999.[129] They demonstrated that a buffer layer formed by presputtering the substrate in nitrogen plasma can significantly improve the in-plane orientation,[129] producing single-crystal InN, and also discussed the effect of GaN buffer layer on crystalline quality of InN.[130] In 1995–1999, Yamamoto *et al.* performed several works on the epitaxial growth of InN on GaAs substrates by the conventional MOVPE system.[66,154,155,157–159] The nitridation of GaAs substrate was studied by flowing NH_3 at a temperature range of 500–900 °C and formation GaN was confirmed by both elemental and structural analysis. It was found that nitridation plays an important role in the epitaxial growth of InN. A single crystalline InN with wurtzite structure was grown on GaAs(111)B, while zincblende with a small fraction of wurtzite phase was grown on GaAs(100). Compared with the sapphire substrate, the surface morphology of the InN film grown on GaAs was better while electrical properties were poor.[157] A comparative study of MOVPE growth of InN on GaAs(111) substrates using a nitrided or grown GaN buffer layer was also made.[158] The InN film grown on a nitrided GaN buffer shows poor crystalline quality and scattered electrical data while surface morphology is better compared with the InN film grown on a MOVPE grown GaN buffer layer on GaAs(111) substrate.

There have been very few reports about the growth and characterization of InN on InAs substrate. Thermodynamic consideration predicts a much higher N incorporation in InAs and InP compared with that in GaAs and GaP. Yamamoto *et al.* studied the nitridation of the InAs(100) substrate by exposing in a NH_3 flow at a temperature range of 450–600 °C.[160] Neither single crystalline nor polycrystalline of InN was formed, new compounds containing N, In, and As were formed on the nitrided InAs surfaces, and formation of AsN_x and metallic In seemed to be possible. However, Lima *et al.* and Tabata *et al.* successfully carried out some significant works, growth of cubic InN on InAs by using plasma-assisted MBE, in 1999.[161,162] In their studies, a cubic InN layer was grown on the top of InAs(001) buffer layer on GaAs(001) substrate. The growth of the *c*-InN film was initiated by a nitridation of the InAs layer, exposing it to a nitrogen flux at 450 °C, and formation of *c*-InN on nitrided InAs surface was confirmed. One thing should be clarified here that the nitridation effect of InAs by exposing in NH_3 and N_2 plasma is different as explained above, while such difference was not observed in the case of GaAs.[78,154,155] This can be explained that in the case of plasma nitridation formation of single crystalline InN and GaN was possible on InAs and GaAs substrates respectively even at a low temperature. In the case of NH_3 nitridation AsN_x is formed on both the substrates at low temperature, which can be decomposed at high temperature. Due to poor thermal stability high temperature nitridation of InAs was not possible, which caused the existence of AsN_x on the InAs surface, while in the case of GaAs, AsN_x disappeared due to comparatively the higher nitridation temperature (600–900 °C), and caused the formation of single crystalline GaN only.

4. GaP and InP

From the viewpoint of lattice and thermal mismatch, GaP may prove better for the improvement of the InN film quality, having smaller lattice and thermal mismatch with InN than that of sapphire. Lattice mismatch between GaP(111) and *h*-InN is smaller than that between GaAs(111) and *h*-InN; 8% for GaP, 11.3% for GaAs, and 25% for α-Al_2O_3. Therefore, GaP has attracted much attention recently as a promising semiconductor substrate and some significant works on the epitaxial growth of InN on GaP have been carried out successfully.[163–166] Guo *et al.* reported the epitaxial growth of InN on GaP(111) substrate, by microwave-excited MOVPE in 1995.[78] The crystalline structure was wurtzite with an epitaxial relationship of (0001)InN//(111)GaP. They demonstrated that the pretreatment of the substrate by exposing to nitrogen plasma before the growth was essential and that the crystalline quality of the InN film is strongly dependent on the exposing time. Bhuiyan *et al.* successfully obtained a single crystalline InN film on GaP(111)B using conventional MOVPE without nitridation of the substrate surface.[163,164] They also studied the nitridation effects of GaP(111)B substrate by exposing to a NH_3 flow for any possible important role on the grown InN

film. It was found that nitridation carries poor effect on the grown InN film due to the formation of PN_x with GaN on the nitrided GaP substrate surface.[163] Recently, the same group has reported that a single crystalline InN film with an excellent surface morphology can be grown on GaP(111) at high temperature using a new two-step growth method.[165,166]

There have been very few reports about the growth and characterization of InN on InP substrate. Pan *et al.* studied the nitridation of InP(100) surface by N_2^+ ion beam bombardment.[167] They confirmed the formation of thin InN on the nitrided InP surface and that the formation of P–N bonds was not observed. Recently, Bhuiyan *et al.* studied the epitaxial growth of InN on InP(111) substrate using conventional MOVPE.[164] A single crystalline wurtzite InN film on InP(111) substrate was grown successfully when the nitridation of the substrate surface was not made. Nitridation of the InP(111) substrate surface by exposing in a NH_3 flow carries poor effect on the grown InN film due to the formation of PN_x on the nitrided substrate surface, as GaP(111).[164]

5. GaN and AlN

The highest mobility and lowest carrier concentration ($2050\ cm^2/V\,s$ and $3.49\times10^{17}\ cm^{-3}$) in the MBE InN film reported recently was grown on HVPE grown bulk GaN template by Lu *et al.*[52] They also reported that using a comparatively thicker AlN layer can significantly improve the structural and electrical properties of the InN film.[168] It is believed that an AlN film of better quality can be obtained by growing a thicker film, which can serve as a better foundation for later InN growth. On the other hand, one of the best mobilities in the MOVPE InN, reported by Yamaguchi *et al.* was grown on a GaN layer.[169] They reported that use of GaN for the underlying layer of the InN film was found to lead to structural improvement of the epitaxial inN film. Recently, Xu *et al.* have investigated the rf-MBE growth of InN on GaN templates.[112] They reported that high quality InN films can be grown on a MBE grown N-polarity GaN template. An InN film grown with N polarity on GaN showed a Hall mobility of $800\ cm^2/V\,s$ at room temperature with a background carrier concentration of $2.1\times10^{19}\ cm^{-3}$.[112] Some other groups also have studied the epitaxial growth of InN on GaN.[55,105–107,159] Two-dimensional growth of InN on GaN has been observed by using MBE in spite of about 10% lattice mismatch.[105,106] In the MOVPE growth of InN, Adachi *et al.* however found that InN grown on GaN/sapphire in a reduced pressure and at a temperature above 550 °C has a much higher metallic–In content compared with that nitrided sapphire and other substrates.[159] Surface polarity of GaN and InN are seemed to be responsible for the In drop formation. If high quality InN film can be grown on GaN or AlN, it will be significant in the device applications. For the realization of InN based electronic devices, the use of high-temperature deposited GaN (high-quality GaN) is essential, and only GaN has the required high quality among nitride semiconductors for device fabrication.

6. Other substrates

Several other materials have also been used as a substrate for the epitaxial growth of InN. These include $MgAl_2O_4$, quartz, glass, metallic substrates, etc. The InN films grown on quartz, glass, metallic substrates, etc. were poor and these materials had been widely used as a substrate in the early days. Recently, Tsuchiya *et al.* reported the epitaxial growth of InN on $MgAl_2O_4(111)$ substrate, and also investigated the initial stages of the InN growth compared with sapphire substrate.[84,85] Lithium salt substrates, such as Lithium gallate ($LiGaO_2$), have been studied as a promising substrate because of its close lattice match with III–nitrides. They have the smallest lattice mismatch to III–nitrides of any commercially available substrate. Growth of GaN on $LiGaO_2$ substrate has been investigated.[170–173] However, growth of InN on $LiGaO_2$ has yet to be reported.

B. Buffer layers

The two-step growth method or growth using buffer layer has now become a standard method for the heteroepitaxial growth of thin films. This method is commonly used to alleviate lattice mismatch and thermal expansion coefficient difference between the substrate and epilayer. In this method, a thin buffer layer is grown at a low temperature in the first step. The main epilayer is grown in the second step at a high temperature. The buffer layer provides the high density of nucleation centers and promotes the lateral growth of the main epilayer. The structure of the low temperature buffer layer is columnar due to islandic growth. Due to the large difference in the lattice constants of the buffer layer and the substrate, the free energy of the system is lowered if the growth is three dimensional (3D). The islands formed in the 3D growth are coherent with the substrate. The time of ramping and annealing the buffer layer has a large influence on the structure of the buffer layer and on the quality of the main epilayer grown subsequently. The two-step growth of InN is not well studied, especially in the MOVPE growth, while two-step growth of GaN is well studied and is a mature growth technology to obtain high quality GaN film. Most of the recent exciting results obtained in the MBE grown InN films use buffer layer technology. Mamutin *et al.* demonstrated that high temperature annealing of a 15 nm thick InN buffer layer grown at low temperature results in significantly improved structural properties of the following InN layer on sapphire substrate.[174] Saito *et al.* showed that combination of a low temperature buffer layer and successive annealing was effective in obtaining high quality InN films.[175] They succeeded in growing InN film two dimensionally with a high mobility by rf-MBE using a low temperature grown InN buffer layer.[176] They also showed that in addition to the low temperature InN buffer layer, incorporation of intermediate layer was effective to obtaining high quality thicker InN films.[177] Using low temperature buffer layer and intermediate layers of InN as shown in Fig. 14, they obtained thicker InN film with uniform surface morphology by rf-MBE. The room temperature electron mobility obtained in the InN grown film as shown in Fig. 14, was $830\ cm^2/V\,s$ and the corresponding carrier concentration was $1.0\times10^{19}\ cm^{-3}$. The room tem-

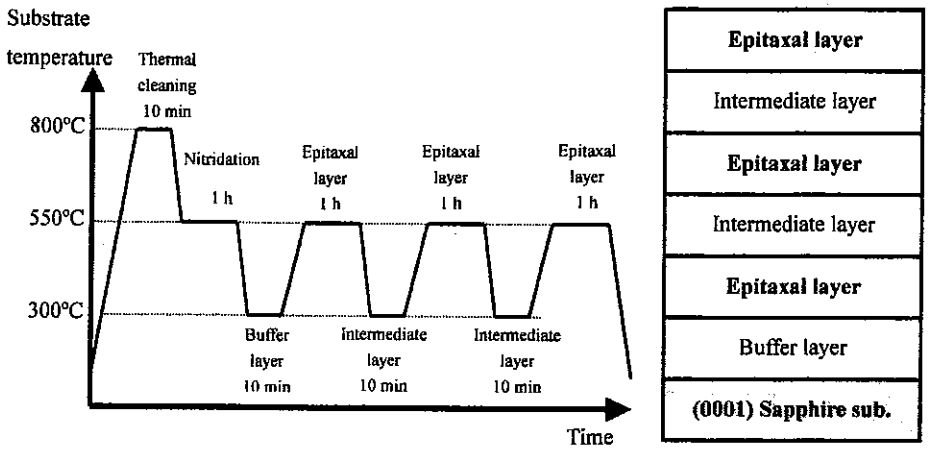

FIG. 14. Growth time chart and structure of InN for obtaining high quality InN using low temperature intermediate layers (Ref. 177).

perature electron mobility obtained in the InN film grown without intermediate layer was 150 $cm^2/V\,s$ and the corresponding carrier concentration was 4.2×10^{20} cm^{-3}.[177] Lu *et al.* reported that using an AlN buffer layer can significantly improve the structural and electrical properties of the InN, that is, with increasing thickness of the AlN buffer layer, the Hall mobility of InN monotonically increases while the electron carrier concentration decreases, and the surface morphology of the film also improves.[168] They also have found that under optimum growth condition, by using an AlN buffer layer, InN film with comparable quality can be achieved by the conventional MBE technique compared to the InN grown by migration-enhanced epitaxy. This result is more important, because it strongly suggests that the improvement of the film quality does not so much depend on the growth mechanism but strongly depend on the surface morphology and the crystal quality of the AlN buffer layer. Recently, Higashiwaki and Matsui reported that the structural and electrical properties of InN films were greatly improved by employing a buffer layer formed with a low temperature grown GaN intermediate layer and a low temperature grown InN layer.[178,179] They showed that a buffer layer formed with a low temperature (LT)-GaN intermediate layer and a LT-InN layer is more effective than only a LT-InN buffer layer. The Hall mobility and carrier concentration at room temperature were 545 $cm^2/V\,s$ and 5.9×10^{18} cm^{-3} for the InN film grown with a LT-InN only, and were 1420 $cm^2/V\,s$ and 1.4×10^{18} cm^{-3} for the InN film grown with a buffer layer formed with a LT-GaN intermediate layer and a LT-InN layer.[179] The above results confirm that the buffer layer technology results in great improvement in the InN film quality also.

There are very few studies about the MOVPE growth of InN using buffer layer, and most of them used a low temperature InN layer as a buffer layer. There is no significant report that use of low temperature InN buffer layers in the MOVPE growth InN gives improvement, like in the case of MBE. It is known that growth temperature can be lowered in the MBE compared with the MOVPE. Pan *et al.* studied the two-step growth of InN using conventional MOVPE.[151] Based on their findings, they concluded that the two-step growth is not adequate for InN, which may correlate to the unstable nature of the InN film. Guo *et al.* reported that if a single crystalline InN film is heated above 550 °C in a N_2 flow, the surface undergoes a considerable change, owing to the decomposition and desorption of nitrogen.[74] In order to suppress the decomposition of InN buffer layer during increasing the temperature, Bhuiyan *et al.* have proposed a new two-step growth technique.[165,166] There are reasons and good indications for potential of improvement of the epitaxial film quality using buffer layer technology. Guo *et al.* reported that as-grown InN film can be significantly improved by thermal annealing at temperatures of 450–500 °C within 10 min in nitrogen ambient.[77]

IV. STRUCTURAL AND CHEMICAL PROPERTIES

A. Crystalline structure and quality

Juza and Hahn first reported the crystalline structure of InN to be wurtzite having lattice parameter $a=3.53$ Å and $c=5.69$ Å.[23] However, the lattice parameter in the rf-sputtered InN film measured by Tansley and Foley, $a=3.548$ Å and $c=5.760$ Å,[12] show a c-lattice parameter much longer than the other reported values and even differ with the lattice parameter measured in the rf-sputtered InN film by Kubota *et al.*, $a=3.540$ Å and $c=5.705$ Å.[46] The crystalline quality of the InN film obtained by Kubota *et al.* was comparatively better than the other previously reported InN films and the lattice parameter is very much closed with the lattice parameter measured in the single crystalline InN film. For example, the lattice parameter measured recently by Davydov *et al.* in the high quality hexagonal InN film was found to be $a=3.5365$ Å and $c=5.7039$ Å.[15] The lattice parameter for polycrystalline and single crystalline InN reported by some authors is plotted in the Fig. 15. The variation in the a-lattice parameter is very little and all the values are quite close and are in good agreement with the theoretical values scattered in the range of $a=3.501$–3.536 Å.[180] The variation in the c-lattice parameter is also samll and all the values are quite close except that measured by Tansley and Foley which is longer than the other measured values in the high quality single crystalline InN film (scattered in the range of $c=5.69$–5.705 Å)[49,169,177] and the theoretical reported values (scattered in the range of $c=5.540$–5.709 Å).[180] The probable reason for the variation is seemed to be due to variation in crystalline quality and

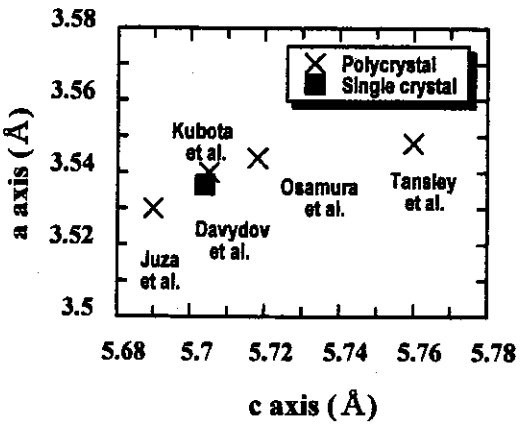

FIG. 15. The lattice parameter for polycrystalline and single crystalline InN reported by different authors.

incorporation of oxygen contamination.[181] Strite *et al.* reported the growth of zincblende InN and measured a lattice constant of 4.98 Å by XRD.[156] Lima *et al.* also reported the growth of zincblende InN film and showed a lattice constant of 4.98 Å measured by XRD, while the value was found to be 5.04 Å when measured from the reflection high energy electron diffraction (RHEED) pattern.[161] Recently, Bhattacharya *et al.* reported the observation of zincblende phase in InN thin film grown by PLD and measured a lattice constant of 5.09 ± 0.04 Å.[145] All these measured values are in good agreement with the theoretical reported values scattered in the range of 4.92–4.98 Å.[180]

Yamaguchi *et al.* characterized the detailed structural properties of the MOVPE grown InN film by triple-axis XRD analysis in terms of lattice mismatch dependence and InN film thickness dependence.[169] Figure 16 shows the $\Delta\omega_c$ and $\Delta 2\theta_c$ as function of (a) lattice mismatch and (b) InN film thickness. For study of the lattice-mismatch dependence, growth of InN film on GaN, AlN, directly on sapphire substrates was performed, and accordingly, $\Delta\omega_c$ was found to range from about 500 to 4000 arsec and $\Delta 2\theta_c$ from about 400 to 700 arsec. Among those three kinds of sample, InN film grown on GaN showed the smallest $\Delta\omega_c$ and $\Delta 2\theta_c$ values. On the other hand, InN thickness dependence of XRD showed that $\Delta\omega_c$ was changed from about 700 to 500 arsec, and $\Delta 2\theta_c$ from about 600 to 300 arsec with increasing InN thickness from 400 to 2400 Å. Moreover, it was found that InN films less than 1200 Å thick are composed of grain islands with different crystalline orientation and that the growth mode changes at a thickness of about 1200 Å and screw dislocations occur. In the above studies the effect of growth condition is not reflected. Lu *et al.* showed that the FWHM of the InN (0002) peak in the XRD θ–2θ scan and ω scan nearly continuously decreases with increasing the temperature.[108] The improved crystal quality may be due to the annealing process occurring at high temperature. In addition to that, they also showed that use of a thick AlN buffer layer in the MBE growth of InN on sapphire substrate significantly improved the structural and electrical properties.[168] Accordingly, the FWHM of the InN (0002) peak in the XRD θ–2θ and ω scans reduces from 7.9 and 43.3 to 7.2 and 24.1 arcmin, respectively, when the AlN buffer layer thickness was increased from 3 to 120 nm. Yang *et al.* recently reported that MOVPE grown InN film quality is markedly improved using a high speed reactant gas.[72]

B. Crystalline defects

Ng *et al.* recently studied the evolution of strain in the InN epitaxial film grown on GaN (0001) by plasma-assisted MBE.[105] The calculated critical thickness for dislocation formation in their InN/GaN is indeed less than 1 BL. Lee *et al.* investigated the evolution of strain in the InN epitaxial film grown on sapphire by a dc faced magnetron sputtering deposition method.[131,133] They showed that film thinner than ~170 Å should be highly strained. The strain was relieved as the film thickness increased, while columnar seeds started to nucleate on parts of the film. The strain in InN film was relaxed completely when the film thickness was thicker than ~450 Å.[133] Yamaguchi *et al.* however found that the residual strain in the MOVPE grown InN film over 1200 Å thick was gradually released.[169] They explained that the improvement in the crystal quality is related both to dislocation density and to the reduction in the degree of misorientation which is present in the InN film. Look *et al.* measured the dislocation density in an InN film grown on a thick AlN buffer layer on sapphire substrate.[182] For this particular material, transmission electron microscopy (TEM) measurements, shown in Fig. 17, find about 3×10^{10} cm^{-2} edge dislocations, and 2×10^{10} cm^{-2} screw and mixed dislocations. The total concentration of threading dislocations in the InN layer is about four times higher than that in the AlN buffer layer, which is unexpected since the AlN/Al_2O_3 lattice mismatch is not much different than the InN/AlN mismatch (~12%–13%). Thus, other factors, such as interface impu-

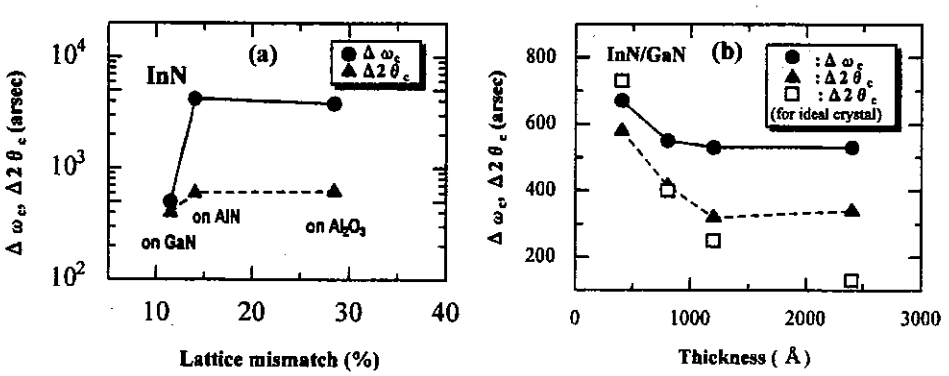

FIG. 16. $\Delta\omega_c$ and $\Delta 2\theta_c$ as function of (a) lattice mismatch and (b) InN film thickness. The reflection surface was (0002). Closed circles denote $\Delta\omega_c$ and closed triangles $\Delta 2\theta_c$. Open squares in the (b) depict $\Delta 2\theta_c$ for ideal crystal (Ref. 169).

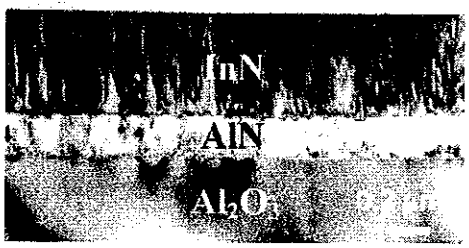

FIG. 17. Cross-sectional transmission electron microscope image of a MBE-grown InN layer (Ref. 182).

rities, may generate further dislocations. In the case of InN film grown on cubic substrate, the interface becomes highly defective due to presence of both cubic and hexagonal domains. Strite *et al.* characterized the microstructure of the heterointerface of a zincblende polytype InN film grown on vicinal GaAs (100) substrate by TEM.[156] They showed that the InN film grown on vicinal (100) GaAs was highly defective with both zincblende and wurtzite domains being present, and a high density of stacking fault defects was observed from which wurtzite domains of InN were nucleated.

C. Polarity study

Grown III–nitrides have a polar configuration, i.e., either group III atoms or N can occupy the first atomic layer. In general, group III terminated plane is denoted as (0001) $(+c)$ or $(111)A$ and group V terminated plane is denoted as (0001) $(-c)$ or $(111)B$. Investigation has shown that these two polar films have vastly differing growth and surface. In addition to that, the polarity also has significant effects on the electrical and optical properties of the film. A variety of other properties of the material also depend on its polarity, for example, etching, defect generation and plasticity, and piezoelectricity. The polarity of GaN has been widely studied and it is found that the polarity of the epilayer is a key parameter for obtaining smooth and low defect density film. Generally, the N-terminated GaN epilayer is found to show a rough surface morphology comprising pyramidal grains and extended defects. While, Ga-terminated GaN film has an atomically flat surface.[183] It is found that the substrate surface and its treatment such as nitridation, buffer layer material and growth condition such as V/III ratio are very important to control the polarity of the grown film.[184] Onozu *et al.* studied the molecular dynamics (MD) simulations to investigate the heteroepitaxial growth process of InN thin film on the polar GaN surfaces.[185] The MD results suggest that the growth of InN thin film on Ga- and N-terminated surfaces is different. On the N-terminated surface, the surface morphology of the grown InN layer is three dimensional and rough. On the other hand, on the Ga-terminated surface, it was observed that the InN molecules have adequate migration mobility for growth and this suggests that the growth follows the two-dimensional growth mode. The above different crystal growth mechanisms were interpreted from the viewpoint of the atomic interaction. At an interface between GaN and InN, the strongest possible bond is the bond between N of InN and Ga of GaN substrate. This is possible only in the case of the Ga-terminated surface. Due to the strong atomic interaction between N and Ga, uniformly deposited InN molecules on the GaN substrate from a regular point of the emitting source are inclined to adhere directly to the substrate instead of aggregating. On the other hand, on the N-terminated surface, In of InN bonds to N of GaN substrate, so that the aggregation of InN molecules causes a three-dimensional growth. Saito *et al.* evaluated the polarity of single-crystalline InN using coaxial impact collision ion scattering spectroscopy.[111] They showed that the polarity of the rf-MBE grown InN on sapphire is very sensitive to the growth temperature. The polarity of the low temperature grown InN was found to be mainly N polarity, that of high temperature grown InN was found to be mainly In polarity, and that of two-step grown InN was found to be a mixture of In polarity and N polarity. Recently, Xu *et al.* reported that InN films grown on nitrided sapphire substrate or N polarity GaN templates were found in N polarity by coaxial impact collision ion scattering spectroscopy.[112]

D. Chemical properties and etching

There have been several studies which report rapid dissociation of InN at temperatures above 500 °C. Trainor and Rose studied the thermal annealing of their InN samples grown by reactive evaporation. All the samples decomposed in a few minutes leaving an indium residue when heated in N_2 (standard pressure) at a temperature 500 °C.[31] They however showed that if the samples were heated in an atomic nitrogen atmosphere (10^{-3} Torr) they did not decompose. Guo *et al.* examined the thermal stability of single crystalline InN film. They showed that if the InN film is heated at a temperature above 550 °C, the surface undergoes a considerable change, owing to the decomposition and desorption of nitrogen.[74]

Indium strongly chemisorbs molecular oxygen. Hence, it is expected that oxidation would occur in preference to nitridation, because of the large difference in the heat formation of InN ($34\ \text{kcal mol}^{-1}$) compared with In_2O_3 ($221\ \text{kcal mol}^{-1}$). Foley and Lyngdal studied the surface oxidation of InN when exposed to ambient.[43] It was found that the surface oxidation of InN was clearly dependent on the aging and sample treatment history. The first stage of oxidation is the bonding of oxygen onto nitrogen to form an In–NO complex. After sputtering etching or abrasive cleaning, the In–NO complex further oxidized to form an $In-NO_2$ complex. The final oxidation state after aging was found to be dependent on the sample preparation condition. Westra *et al.* studied the effects of oxygen contamination on the properties of reactively sputtered InN film.[44] They found bulk oxygen impurity concentration of at least 11% in the InN film deposited by reactive dc planar magnetron sputtering. In spite of this bulk contamination, the crystal structure showed no evidence of In_2O_3 or of an indium oxynitride. They proposed that the oxygen forms an amorphous indium oxynitride that exists in an InN polycrystalline matrix. The oxygen or oxynitride centers could act as a scattering center, causing mobility reduction, and also as a dopant, increasing the electron concentration. There are also some other reports

where oxygen is discussed as a potential candidate for the high concentration of donors in the InN. Recently, Motlan *et al.* reported that physisorbed oxygen is eventually chemisorbed into the InN film due to aging and annealing treatments, converting them into an oxynitride (InON) phase.[134] This is observed through the increase of the band gap energy by about 0.2 eV in the sample aged for 6 months and even greater increase of 0.8 eV in the sample annealed at 400 °C.

While progress has been made in improving the InN film quality, there is still a long way to go in developing process modules for device fabrication. Recent advances in the epitaxial growth of InN suggest that the processing technology will shortly become of great importance. In order to realize device application of InN, a reliable pattern transfer technology must be established. To achieve that goal, several studies have been reported on the wet and dry etching of InN. The wet etching of the III–nitrides was proven difficult due to their low chemical reactivity while dry etching resulted in low rates and also can induce damage. Guo *et al.* reported the wet etching of InN and showed that acid solutions are inappropriate for etching the InN surface,[186] while alkaline etchants, such as aqueous KOH and NaOH solutions, give controllable etching rates and they obtained smooth surface free from etch pits. Mileham *et al.* also reported that no measurable etching was observed in all of the common acid solutions. They showed that KOH-based solutions attack the interfacial region between InN and GaAs causing liftoff of the epitaxial InN layer, most likely due to defective interfacial region between the two semiconductors.[187] Pearton *et al.* however obtained a very slow etching rate (~10 Å/min at room temperature) of InN even in acid solution (1:1 HCl/HNO_3).[188] Recently, Ohkubo and Takai studied the photoassisted anodic wet etching of InN in a mixture of a buffered aqueous solution of tartaric acid and ethylene glycol.[189] They showed that etch rate increases with current density and the highest rate is obtained when the *p*H of the electrolyte was 7.0. The etching rate obtained by the above wet etching techniques is about few hundred angstroms per minute. There are also few studies on the dry etching of InN. Pearton *et al.* examined the dry etching characteristics of InN using CCl_2F_2/Ar, BCl_3/Ar, and $CH_4/H_2/Ar$ discharges.[188] The etching characteristic of InN is similar in CCl_2F_2/Ar and BCl_3/Ar mixtures. The etching rate increases in an essentially linear fashion with dc bias in all the three mixtures. However, slow and smooth etching of InN is achieved with the $CH_4/H_2/Ar$ chemistry and also there is some selectivity for the etching of InN over some materials, e.g., AlN, Al_2O_3, GaAs, etc. which would be required in the device fabrication. They also showed that the chloride-based discharge chemistry is not effective for InN, as etch product $InCl_x$ species are not available near room temperature.[190] As with InP and related compounds, CH_4/H_2 should work well for InN by forming volatile $(CH_3)_xIn$ and NH_3 etch products. Accordingly, they successfully obtained highly anisotropic dry etching of InN at low dc self-bias in ECR $CH_4/H_2/Ar$ discharges with an etch rate of ~350 Å/min.[190] Shul *et al.* studied the high-density plasma etching as a function of plasma chemistry, cathodic rf-power, inductively couple plasma (ICP) power, and chamber pressure.[191] They however showed that under high dc-bias condition fast InN etch rate (~5500 Å/min) can be obtained in a Cl_2/Ar plasma at 2 m Torr chamber pressure, 500 W ICP source power, and 25 °C cathode temperature. This was significant as the etch product $InCl_3$ has a low volatility and typically requires high etch temperature to increase the volatility and yield reasonable etch rate. Faster rate was attributed to highly efficient breaking of the bonds and sputter desorption of etch products at higher energies. Due to strong bond energies, etching of the III–nitrides requires either high ion energies or high ion flux at energies above the III–N bond breaking threshold energy to achieve reasonable etch properties. Recently, Guo *et al.* studied the characteristics of reactive ion etching of InN layer using CH_4 and H_2 gases.[192] A smooth etched InN surface was obtained in the range of 5%–15% CH_4 concentration and 25–55 Pa pressure. The etching rate of InN increased from 260 to 1310 Å/min with increasing the plasma power from 100 to 300 W at a 10% CH_4 concentration and 45 Pa pressure.

V. ELECTRICAL PROPERTIES

A. Background defects

As-grown InN is always *n*-type with a very high background carrier concentration-an observation similar to GaN before better doping control of that material was achieved. However, there is only one report of *p*-type InN grown by the PLD technique, which to date has never been reported in as-grown InN film or even intentionally doped InN film. There has been much speculation as to what species is responsible for high background donor concentration in the grown InN. Theoretical calculation as well as experimental result gives conflicting views and opinions regarding the major reason responsible for such high *n*-type conductivity. The potential candidates for such high background donors are native defects, such as N vacancy, nitrogen antisite, and impurities, such as O_N, Si_{In}, and possibly interstitial H. According to the oldest and common view, the nitrogen vacancy is the most probable reason for *n*-type conductivity of InN. Tansley and Foley had speculated that the *n*-type behavior is caused by an antisite defect: N on an In site (N_{In}), which they had suggested might be a double donor.[40] Jenkins and Dow have carried out an extensive study about the native defects (i.e., vacancies and antisite defects) and impurities in InN.[193] They showed that the native defect responsible for naturally occurring *n*-type InN is a nitrogen vacancy, neither antisite defect can explain the observed *n*-type character of InN. Another defect possibly responsible for the *n*-type character of InN is oxygen on a N site, which is not a native defect, but is nevertheless likely to be present in significant concentration. It is most likely that every nitrogen vacancy donates a single donor but possibly donates three electrons to the conduction band.[193] Tansley and Foley have also speculated that the N vacancy might be the defect responsible for natural *n*-type character of InN.[121,122] According to their study, both experiment and theory point to a triplet of donor states associated with the nitrogen vacancy, with deep compensating centers deriving from antisite defects. The ionic radius of the metal then seems to determine the conductivity

of as-grown material, indium is reluctant to occupy nitrogen sites while aluminum does so readily and gallium is equivocal. Thus the upper donor level of InN is not depleted and n-type behavior is always observed. There is also a simple approach to how the nitrogen vacancy contributes a donor in the as-grown InN film. The donor nature of the N vacancy is constructed as a missing N atom surrounded by four In atoms that provide three valence electrons to complete the bonding octet with the five missing electrons of nitrogen. Two of these three electrons would be donated to the conduction band. Therefore, it has been believed that nitrogen vacancy is the dominant donor in the as-grown InN film. There is much experimental evidence supporting this view. For example, the carrier concentration decreases and Hall mobility increases with increasing NH_3/TMI molar ratio in the MOVPE grown InN film.[63] In addition, enhancement of NH_3 decomposition in the MOVPE InN gives better electrical properties.[51] In contrast with the above views, there are also some theoretical as well as experimental evidence, which argues against the nitrogen vacancy being responsible for the background n-type conductivity. Stampfl *et al.* performed first-principles density-functional calculation to investigate the electronic and atomic structure and formation energies of native defects and selected impurities (O, Si, and Mg) in InN.[194] Their calculation showed that neither vacancy nor antisite can explain the observed n-type conductivity of InN. Therefore, oxygen and silicon impurities were examined, finding that they act as donors and that they can easily be incorporated during growth. Recently, Look *et al.* presented a formalism to determine donor and acceptor concentrations in degenerate InN.[182] From a comparison with glow discharge mass spectroscopy measurement and the developed theory, they suggested that a potential candidate for the dominant donor in InN is H. However, the native defects also cannot be completely ruled out. As discussed above both theoretical calculation as well as experimental result gives conflicting views and opinions regarding the major reasons responsible for high n-type conductivity of as-grown InN film. However, on the basis of the data discussed here and available in the literature, two major reasons can be concluded. One is native defects, mainly nitrogen vacancy, and one is impurities, mainly oxygen. There is contradiction about nitrogen vacancy but about oxygen there is no contradiction as it can act as a donor.

B. Hall mobility and electron concentration in undoped InN

The carrier concentrations and Hall mobilities reported for undoped InN film grown by a variety of techniques are plotted against the calendar year in Figs. 18 and 19, respectively. The growth methods are divided into five categories: MBE, MOVPE, HVPE, sputtering and others, including electron beam plasma method, reactive evaporation and pulsed laser deposition. Until the 1980s most of the InN films were deposited using sputtering. The grown films were polycrystalline with a carrier concentration scattered from 10^{18} to 10^{21} cm^{-3} and Hall mobility from 20 to 250 $cm^2/V\,s$ with the exception of Tansley and Foley. They attained a dramatic reduction of the carrier concentration with very high electron mobility.[38] A room temperature carrier concentration of 5×10^{16} cm^{-3}, which decreased to a minimum of 3×10^{16} cm^{-3} at 150 K, was measured. As a result, a room temperature electron mobility of 2700 $cm^2/V\,s$, which reached a maximum value of 5000 $cm^2/V\,s$ at 150 K, was measured. These are the best electrical properties ever achieved in InN, and is all the more impressive given that the InN was polycrystalline. Unfortunately, the InN film prepared by reactive sputtering in other laboratories has not met these expectations and has universally high carrier concentration near 10^{20} cm^{-3} and constantly low electron mobility of less than 100 $cm^2/V\,s$. The InN film grown by different other techniques also suffered from high carrier concentrations and constantly low electron mobility.

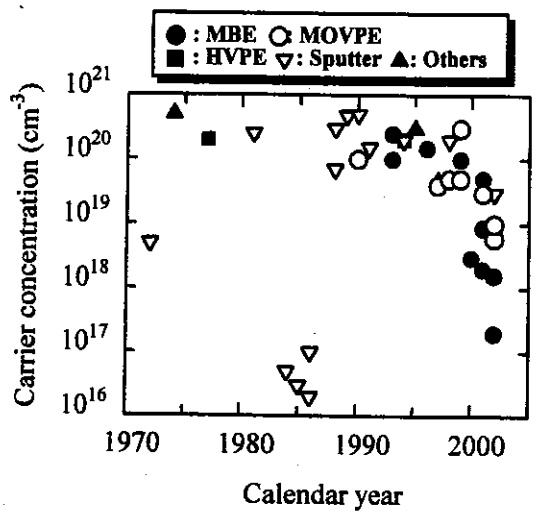

FIG. 18. Carrier concentration reported for undoped InN film grown in a variety of technique is plotted against the calendar year.

Sato achieved a carrier density of 4×10^{19} cm^{-3} in the InN epitaxial layer grown on sapphire substrate by plasma-assisted MOVPE in 1997.[81] However, there is no further improvement or report on the electrical properties of InN by plasma-assisted MOVPE. On the other hand, significant im-

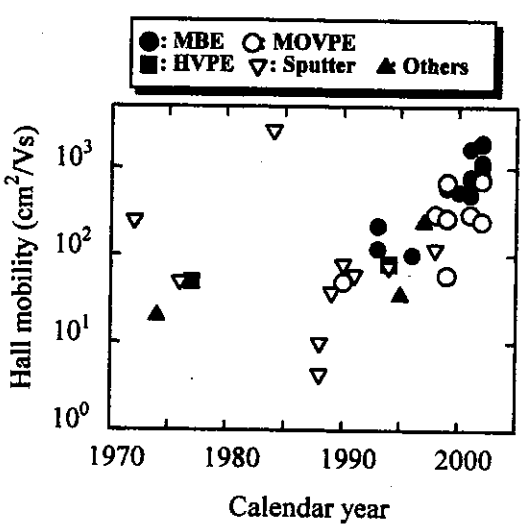

FIG. 19. Hall mobility reported for undoped InN film grown in a variety of technique is plotted against the calendar year.

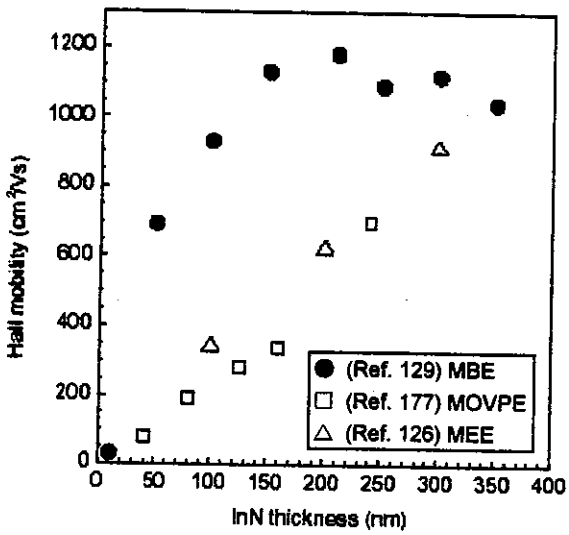

FIG. 20. Room-temperature Hall mobility as a function of InN thickness in InN films grown by MBE, MOVPE, and MEE (Ref. 178).

provement in the conventional MOVPE grown InN film was started since the work of Yamamoto *et al.* and Pan *et al.* where they reported an electron concentration of 5×10^{19} cm^{-3} with a Hall mobility of about 300 cm^2/V s in the InN film grown on sapphire substrate.[66–151] Yamaguchi *et al.* showed that selection of GaN for the underlying layer and increased InN film thickness significantly improve the Hall mobility. A Hall mobility of about 700 cm^2/V s was obtained in the InN film grown on GaN even at an electron concentration of 5×10^{19} cm^{-3}.[169] Yamamoto *et al.*[51,63,66] showed a high NH_3/TMI molar ratio and enhanced NH_3 decomposition (by growth temperature, atmospheric pressure growth, reduced flow velocity, etc.) significantly improved the electrical properties of MOVPE grown InN film. As a result, a carrier concentration in the order of 10^{18} cm^{-3} was obtained and the highest electron mobility obtained was 730 cm^2/V s. These are the best electrical properties ever achieved in the MOVPE grown InN film. Laser-assisted MOVPE has the potential to decompose NH_3 photolytically independent of the substrate temperature.[87] Lu *et al.*[108] obtained an electron concentration of 3×10^{18} cm^{-3} with a Hall mobility of 542 cm^2/V s in the InN film grown by MEE. They also showed that the Hall mobility for both growth methods, MEE and MBE, increases with film thickness. Similar thickness dependence in Hall mobility was also observed in the MOVPE grown InN film.[169] The thickness dependence of the mobility is presumed to be reduced defect density away from the lattice-mismatched substrate. However, Higashiwaki and Matsui found that the there was an immediate sharp increase in mobility up to a film thickness of 150 nm, beyond which it almost leveled out.[178] The room-temperature Hall mobility as a function of InN thickness in the InN film grown by MBE, MOVPE, and MEE is shown in Fig. 20. Recently, Lu *et al.* have achieved a carrier concentration in the order of 10^{17} cm^{-3} and a mobility of more than 2000 cm^2/V s in the thick InN film grown on HVPE grown bulk GaN template.[52] The use of a buffer layer of AlN, GaN or InN seems to contribute the improved structural and electrical properties of MBE grown InN. The better electrical properties in the MBE InN film compared with the MOVPE are believed to be due to that active nitrogen can be supplied independent of the growth temperature and reduced impurity incorporation in the MBE growth.

C. Doping in InN

Since the undoped InN film usually demonstrates high n-type conductivity, the doping of InN has not attracted much interest yet. Jenkins and Dow have studied theoretically about the suitable dopants for both p-type and n-type InN.[193] If InN is naturally n type because of nitrogen vacancies, then p-type material must relatively free of vacancies or contain a sufficiently large number of acceptors to compensate them. Column IV impurities on the N site will very likely not produce shallow acceptors. They also noted that the In vacancy could dope InN p type. For n-type doping, they predicted the best candidate other than the N vacancy is oxygen or some other chalcogen on a N site. Column IV impurities on the In site are not good candidates for donors. Mamutin *et al.* attempted Mg doping of hexagonal InN film grown on sapphire by plasma-assisted MBE.[195] p-type InN was not obtained but significant improvement of InN:Mg crystal quality in the Mg concentration range of 10^{19}–3×10^{20} cm^{-3} was observed, which is most likely due to a Mg surface segregation. Increase of Mg doping level over 10^{21} cm^{-3} deteriorates the InN crystal quality and surface morphology, causing a large concentration of Mg interstitials. The heavy Mg doping results in an order of magnitude reduction of electron concentration in InN, but complete compensation was not achieved. Lu *et al.* also attempted Mg doping of InN but was unsuccessful.[196] Usually more electrons were created when more Mg was added. Higher Mg flux resulted in higher defect densities, and hence, higher electron concentrations due to defects.

VI. OPTICAL PROPERTIES

A. Optical band gap energy

Related to optical properties of InN, an exciting conflict has recently arisen about one of the basic physical properties of InN, the optical band gap energy. This conflict was raised recently when a few groups showed by PL measurement that the band gap energy of InN is in between 0.65 and 0.90 eV,[15–22] which is much smaller than 1.89 eV,[12] the most commonly accepted value. The band gap energy values reported for InN films are plotted as a function of carrier concentration, as shown in the Fig. 21. It has been a mystery even recently that no photoluminescence spectrum could be observed for InN, even though it is predicted as a direct band gap material with the gap energy of about 1.89 eV, except the one of Yodo *et al.*[54] The absorption edge or optical band gap energy has been primarily determined by optical absorption or transmission measurements. Osamura *et al.* performed optical absorption measurements near the fundamental absorption edge for polycrystalline thin films of the alloy of InN and GaN grown by electron beam plasma technique over the entire composition region.[33,34] They determined the band gap energy of InN to be 1.95 eV at room temperature and to be

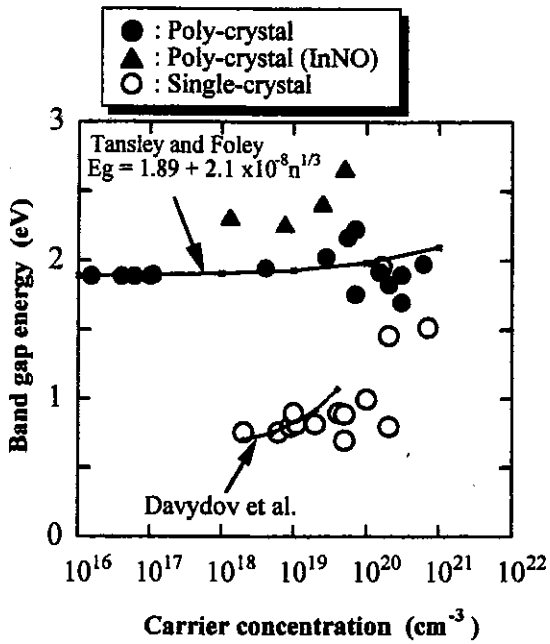

FIG. 21. Band gap energy for InN films as a function of carrier concentration.

2.11 eV at 78 K. Some other groups also reported similar values of band gap energy, around 2 eV, measured by optical absorption in the polycrystalline InN film.[35,37] Later, Tansley and Foley measured a fundamental absorption edge at 1.89 ±0.01 eV in high purity InN films grown by reactive sputtering.[12] They also measured the infrared (IR) absorption of InN and observed an unidentified donor level approximately 50–60 meV below the conduction band edge.[42] The measured band gap, i.e., 1.89 eV, has been the most commonly accepted and referred band gap value of InN. There are also some other reports which support this value for the band gap of InN measured by optical absorption even for single crystal InN film.[76] In 2001, Yodo *et al.* observed strong band edge luminescence at 8.5–200 K from 200 to 880 nm thick InN film grown on Si(001) and Si(111) substrates by ECR-MBE.[53,54] The InN film on the Si(001) substrate exhibited strong band edge PL emission at 1.814 eV at 8.5 K, tentatively assigned as donor to acceptor pair (DAP) emission from wurtzite–InN crystal grains, while those on Si(111) showed other strong band edge PL emission at 1.880, 2.081, and 2.156 eV, tentatively assigned as donor bound exciton (D^0X) from wurtzite–InN crystal grains, DAP, and D^0X emissions from zincblende–InN grains, respectively.

Evidence of a narrower band gap for InN was reported in 2001. Inushima *et al.* insisted that the fundamental absorption edge of MBE grown InN layer lies around 1.1 eV, which is much lower than the previously reported values.[197] Davydov *et al.* reported a band gap value of 0.9 eV for high quality MBE grown InN, studied by means of optical absorption, PL, photoluminescence excitation (PLE) spectroscopy, as well as by *ab initio* calculation.[15] Figure 22 shows (a) absorption edge and (b) photoluminescence spectra for MBE grown InN sample with a different carrier concentration. All the data from these measurements consistently showed that the band gap of InN was much less than the previously reported value (around 2 eV). They further studied in detail with different high quality hexagonal InN films grown by different epitaxy methods. Analysis of optical absorption, PL, PLE, and photoreflectivity data obtained on single crystalline hexagonal InN film leads to the conclusion that the true band gap of InN is $Eg \sim 0.7$ eV.[16,20] This finding was supported by optical studies of In-rich $In_xG_{1-x}N$ alloys. Several other groups also have reported that the band gap of InN is less than 1 eV.[17–19,21,22] Wu *et al.* showed good coincidence of data for optical absorption edge, PL peak energy, and photomodulated reflectance for MBE grown epitaxial layers with a carrier concentration of order of 10^{18} cm^{-3} and a mobility higher than 1000 cm^2/V s, which showed an energy gap for InN between 0.7 and 0.8 eV.[17] Matsuoka *et al.* observed at room temperature strong PL at 0.76 eV as well as a clear absorption at 0.7–1.0 eV for the MOVPE grown InN film.[18] In contrast, no PL was observed, even by high power excitation, at ~1.9 eV.

Which value is the true band gap of InN, ~2 or ~0.7 eV? From the standpoint that the larger band gap is correct, the emission at around 0.7 eV is interpreted as a deep emission. From the viewpoint of narrow band gap, the larger band gap cited in the literature may be due to the formation of oxynitrides, which have much larger band gaps than that of InN. As can be seen in Fig. 21, energy gap data less than 1 eV were obtained for single crystalline InN film with a relatively low carrier concentration, while the larger

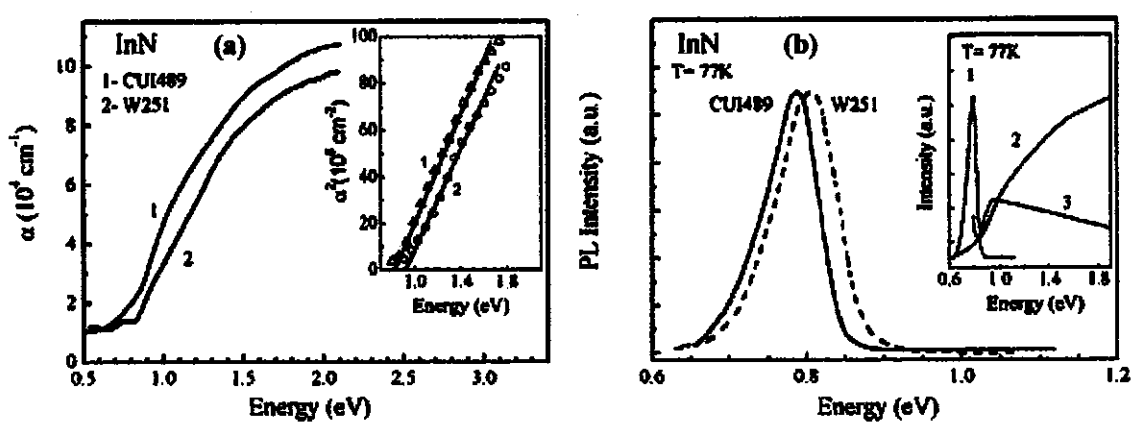

FIG. 22. (a) Absorption edge and (b) photoluminescence spectra for MBE grown InN samples with a different carrier concentration (Ref. 15).

values were mostly for polycrystalline InN film. It should also be pointed out that the band gap obtained from epitaxial films shows a remarkable dependence of carrier concentration, which is different from the larger one obtained from polycrystalline films. Polycrystalline films show a similar band gap (~2 eV) in spite of the wide range variation of carrier concentration 10^{16}–10^{21} cm^{-3}. Thus, these two values, 2 and 0.7 eV, seem to be from different materials. As Motlan reported, oxygen incorporation is one of the cause for the increase in band gap for the larger case.[134] Therefore, the larger values may be related to oxygen incorporation into grown InN because polycrystalline film can contain a high density of oxygen atoms at their grain boundaries. Davydov *et al.* showed that the sample with band gap in the region of 1.8–2.1 eV contained up to 20% of oxygen,[20] much higher than for samples with narrow band gap. It can be assumed that oxygen is responsible for a high concentration of defects. In this case an increase of the band gap in wide gap samples can be caused by formation of oxynitrides, which have much larger band gap than that of InN. On the other hand, in the evidence of narrow band gap by PL measurement, the origin of PL from InN is not so clear. Emission from a deep level also cannot be ruled out. Jenkins and Dow predicted deep levels near mid gap of InN that are responsible for an optical absorption near 1 eV.[193] Tansley and Egan identified five distinguishable defect energy levels observed in the band gap of InN.[121,122] These studies lead to confusion about the evidence for narrow band gap reported recently. Therefore, in order to settle the band gap value of InN, growth of more high quality InN film and further studies on the measurement of optical properties are required. Also previous reports about the ~1.9 eV band gap need to be reexamined.

B. Variation in optical band gap energy

It is well known that the band gap energy of most of the semiconductors generally decreases with increasing temperature. The variation of InN band gap with temperature is studied for both the reported band gap values of ~2 or ~0.7 eV. Osamura *et al.* measured the InN band gap as a function of temperature and obtained a band gap temperature coefficient of $dE_g/(dT) = -1.84\times10^{-4}$ eV/K.[34] Guo and Yoshida studied in detail the temperature dependence of band gap change in InN.[76] The band gap energy of InN single crystal is found to be 1.97 eV at room temperature and varies linearly from room temperature down to about 150 K.[76] The temperature coefficient (dE_g/dT) in this temperature region is approximately -1.84×10^{-4} eV/K. However, for the temperature region below 150 K, the band gap does not change linearly with temperature, and has a very small temperature coefficient. This tendency is similar to that for other compound semiconductors. There are also few studies about the temperature dependence of band gap change in InN by PL measurement in the case of narrow band gap. Wu *et al.* studied the temperature dependence of PL peak energy and intensity.[17] The PL peak energy increased with increasing temperature and the shift was smaller for the sample with high electron concentration. This behavior is in a stark contrast to the temperature dependence of the direct band gap in most semiconductors. They further studied the reasons and found that the intensity of the PL decreases by ~20 times and the FWHM increases from 35 to 70 meV when the temperature increases from 11 K to room temperature. It can be, therefore, concluded that there is no significant shift of the PL spectra, as the temperature-induced line broadening can easily account for the observed small upward shift of the PL line maximum. Davydov *et al.*, however, did not observe such anomalous temperature dependence of the PL band and the band gap was found to be decreased with increasing temperature.[20] For the PL band of InN at 77 and 300 K, the shift is about 23 meV, which can also be related to the temperature-dependent band gap narrowing.

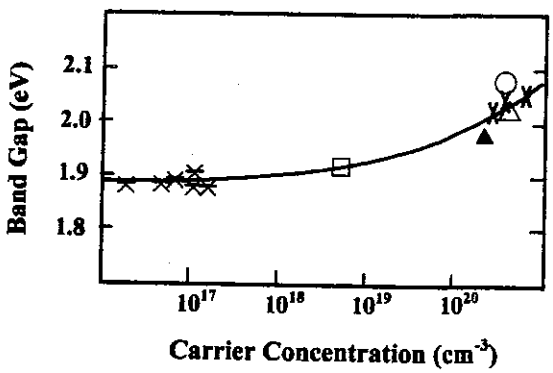

FIG. 23. Band gap as a function of carrier concentration for various InN samples showing a significant Burstein–Moss shift (Ref. 12).

In a degenerate semiconductor, the band edge is expected to shift toward higher energy with increasing carrier concentration (Burstein–Moss effect). The variation of InN band gap with carrier concentration is also studied for both the reported band gap values of ~2 or ~0.7 eV. Trainor and Rose found that increasing absorption edge energy was associated with increasing carrier concentration.[31] This trend of absorption edge with carrier concentration was studied later in detail by Tansley and Foley for the InN film prepared with reactive sputtering.[12] Figure 23 shows the reported band gap values as a function of carrier concentration for various InN samples showing a significant Burstein–Moss shift. Tansley and Foley measured a fundamental absorption edge at 1.89 ±0.01 eV in the high purity InN film grown by reactive sputtering and the Burstein–Moss shift was empirically expressed by

$$E_g = 1.89 + 2.1\times10^{-8}\ n^{1/3} \quad (\text{eV}) \tag{7}$$

for carrier concentration in the range 1×10^{16}–5×10^{20} cm^{-3}, where E_g is optical band gap and n is carrier concentration in cm^{-3}.[12] Davydov *et al.* studied the carrier concentration dependence of band gap change in InN by PL measurements in the case of narrow band gap.[16] Figure 24 shows the (a) semilog PL spectra of InN layer with a different carrier concentration and (b) calculated shift of optical absorption edge due to the Burstein–Moss effect. It can be seen that the absorption edge shifts considerably as carrier concentration increases. The shift of the optical absorption edge of n-type InN due to the Burstein–Moss effect is calculated by

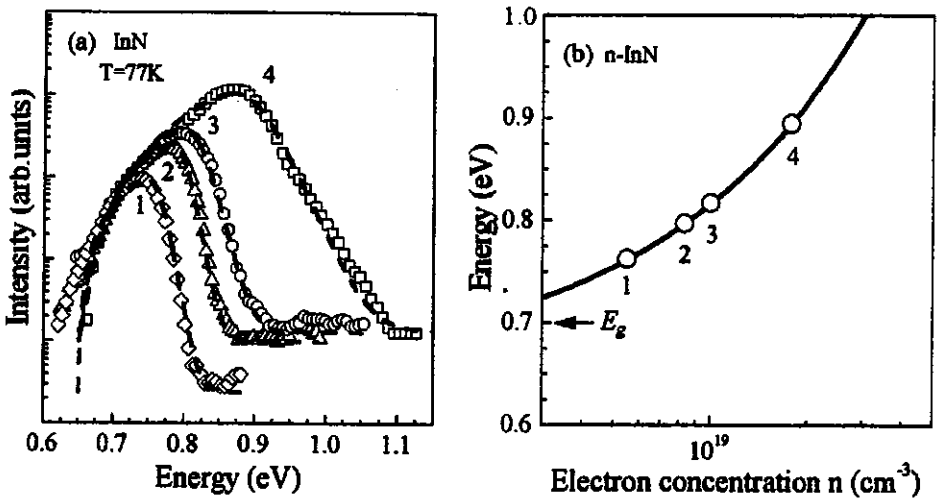

FIG. 24. (a) Semilog PL spectra of InN layer with a different carrier concentration. (b) Calculated shift of optical absorption edge due to the Burstein–Moss effect (Ref. 16).

$$E_g = 0.65 + 0.0166\ (m_0/m^*)(n \times 10^{-19})^{2/3} \quad \text{(eV)}. \quad (8)$$

They also analyzed the shape of PL band with the valence–conduction band transition for heavily doped semiconductors and showed that the shape of the PL band at $\hbar\omega > E_g$ can be described by

$$I(\hbar\omega) \sim [\hbar\omega - E_g]^{\gamma/2} f(\hbar\omega - E_g - E_F), \quad (9)$$

where $I(\hbar\omega)$ is intensity and $f(\hbar\omega - E_g - E_F) = 1/\{\exp[(\hbar\omega - E_g - E_F)/kT] + 1\}$ is a Fermi distribution function. The value $\gamma = 1$ holds if only vertical interband transitions are allowed, or $\gamma = 4$ is valid if the momentum conservation law is completely broken due to the influence of defects and/or impurities on the hole states.

The variation of band gap with film thickness and aging time was also reported recently. Motlan *et al.* reported the optical characterization together with electrical properties of InN thin film prepared by RF reactive sputtering of In target with pure nitrogen.[134] They found that the absorption edge energy was increased with decreasing film thickness and increasing aging time and annealing temperature. Figure 25 shows the variation of the band gap (a) with film thickness and (b) with aging time after the growth. In particular, they obtained an absorption edge as large as 2.8 eV when the film was annealed at 400 °C in nitrogen atmosphere. This increase in the absorption edge was found due to the oxygen incorporation into the film and such a high absorption edge energy of 2.8 eV was caused by the formation of InNO compounds.

C. Raman scattering and IR absorption

Raman scattering and IR absorption have contributed a great deal to the advances in the III–nitrides semiconductor research field. These are convenient and nondestructive methods for the evaluation of crystalline structure, stress, free carrier concentration, quality of the grown semiconductor film, as well as some other important issues. The InN is highly stable in the hexagonal WZ structure. The WZ crystal structure belongs to the space group C_{6V}^4, and the group theory analysis predicts the zone-center optical modes $A_1 + 2B_1 + E_1 + 2E_2$. Among them, the A_1 and E_1 modes are both Raman and infrared active, the two E_2 modes are only Raman active, while the B_1 modes are silent, i.e., forbidden in Raman scattering. The A_1 and E_1 modes are polar: their vibrations polarize the unit cell, which results in the creation of a long-range electrostatic field. The effect of this field manifests itself in the splitting of the A_1 and E_1 modes into longitudinal optical (LO) and transverse optical (TO) components, thus creating the A_1(LO,TO) and E_1(LO,TO) modes. In 1975, Osamura *et al.* measured long-wavelength optical phonons in the polycrystalline InN film using an infrared reflectivity measurement.[34] The reported phonon frequencies were 478 cm^{-1} for the transverse optical phonon and 694 cm^{-1} for the longitudinal optical phonon. Kwon *et al.* studied the Raman spectroscopy of single-crystalline InN film grown by microwave-excited MOVPE and observed two phonon modes: A_1(LO) and $E_2^{(2)}$ modes.[79] Chen *et al.* also found the same two modes in the Raman spectros-

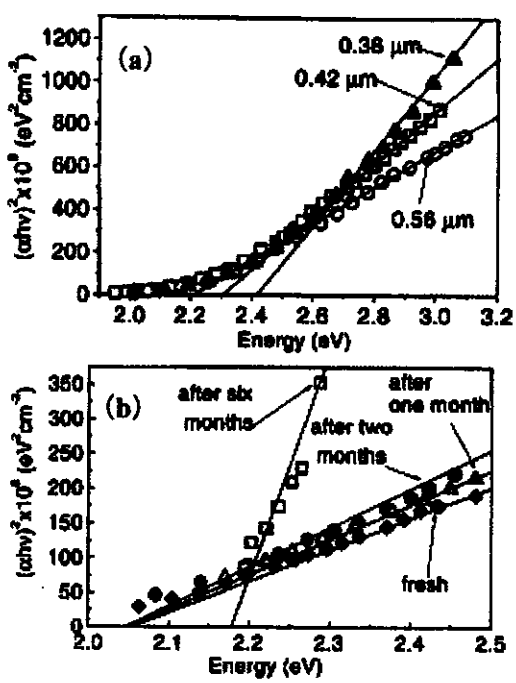

FIG. 25. The variation of the band gap (a) with film thickness and (b) with aging time after the growth (Ref. 134).

TABLE I. Raman data reported for hexagonal InN.[a]

E_2 (low)	B_1 (low)	LOPC (low)	E_1 (TO)	A_1 (TO)	E_2 (high)	B_1 (high)	E_1 (LO)	A_1 (LO)	Ref.
Experimental									
...	...	...	...	...	495	...	...	596	79
...	...	...	...	...	491	...	...	590	153
...	...	...	475	446	488	...	...	574	198
...	...	...	...	...	491	...	...	590	151
87	200	...	476	480	488	540	570	580	199
87	...	450	476	447	488	...	593	586	200
87	...	...	476	447	488	...	593	586	201
82	...	...	...	...	488	...	...	588	174
88	...	...	...	440	490	...	...	590	202
87	...	441	...	...	491	...	...	588	197
...	...	440	...	...	488	...	...	587	114
88	...	450	...	...	490	...	...	590	203
88	...	440	...	...	489	...	...	589	18
88	...	...	...	...	491	...	...	589	21
Theoretical									
104	270	...	472	440	483	530	...	...	198
93	202	...	470	443	492	568	605	589	202

[a] A_1, E_1, B_1, etc. stands for vibrational symmetry. For details see the text on vibrational spectroscopy.

copy of InN film grown by MOVPE with much narrower FWHM of the peaks which reflected the growth temperature dependence of the film quality.[153] The mixing of cubic and hexagonal crystal structures was also detected by Raman spectroscopy in the films grown at low temperature. However, in these studies only two phonon modes were observed. After that many groups reported detailed Raman scattering data for single-crystalline InN films. Table I lists the experimental Raman frequencies that have been reported for hexagonal WZ InN.[18,21,114,151,174,197–203] The theoretical calculations of Raman frequencies for hexagonal InN performed by Dyck *et al.* and Kaczmarczyk *et al.* are also included in the Table I for comparison.[198,202] There are small differences in the Raman frequencies presented in Table I, which in most cases are due to differences in material quality. Inushima *et al.* determined all the phonon energies including the silent modes of single crystalline InN film grown by ultraviolet assisted ALE, as shown in Fig. 26 and the values of the Raman frequencies are listed in Table I.[199] The E_1 modes assigned from the infrared spectra are also shown in the figure by arrows. The back scattering configuration is widely used as the measuring geometry. In this configuration, two E_2 and A_1(LO) modes are obtained with the parallel polarization $z(xx)\bar{z}$, while A_1(LO) mode is suppressed in the crossed polarization geometry $z(xy)\bar{z}$ as shown in Fig. 26. Inushima *et al.* observed two phonon structures at 200 and 540 cm^{-1} in the $z(xx)\bar{z}$ configuration only, and assigned them to be the silent B_1 modes. However, Kaczmarczyk *et al.* interpreted the weak structure around 200 cm^{-1} as second order process of the acoustic phonon and not as the B_1 (low) silent mode, which should be much too weak to be observed.[202] Davydov *et al.* also have measured and assigned all the six Raman active modes in the spectra of InN as listed in Table I, and five of them were observed in the same InN sample grown on sapphire $(1\bar{1}02)$ substrate.[200,201] The Raman spectrum in the $z(xx)\bar{z}$ had a pronounced feature at 445 cm^{-1}. Examination of Mg-doped InN sample showed that this feature shifts towards lower frequencies with decreasing carrier concentration as shown in Fig. 27(a). They assigned this feature to the lower coupled plasmon-LO-phonon mode (PLP^-) arising in polar semiconductors due to interaction of the longitudinal optical modes through the macroscopic field with collective excitations of free carriers. The shift of the IR reflection line caused by plasma oscillations from 3500 to 800 cm^{-1} with increasing acceptor concentration, as shown in Fig. 27(b), supports this interpretation. Therefore, one can estimate electron concentration in the sample with this shift. The evaluation of crystalline quality and strain by Raman spectroscopy were reflected in a recent study of Kurimoto *et al.*[203] A sharp phonon peak was observed in the InN film grown by MOVPE on sapphire substrate, showing good crystalline quality. They showed that the E_2 modes, which are sensitive to the strain in the *c* plane, have a systematic variation in frequency with the growth temperature due to thermal strain induced by the differences in thermal expansion coefficients between the InN layer and the sapphire substrate. The high-frequency E_2 pho-

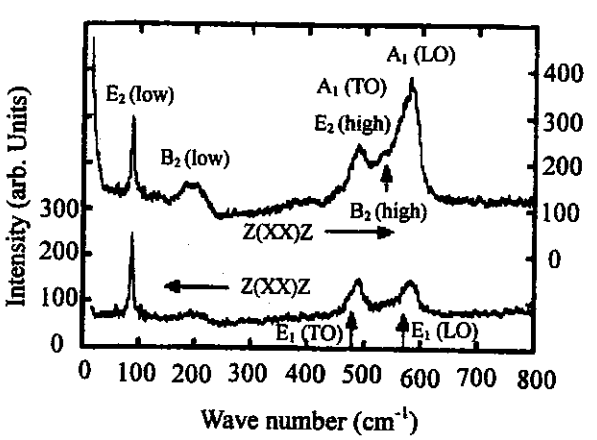

FIG. 26. Raman spectra of InN. The notation indicates the assigned phonon modes. The E_1 modes assigned from the infrared spectra are indicated by arrows (Ref. 199).

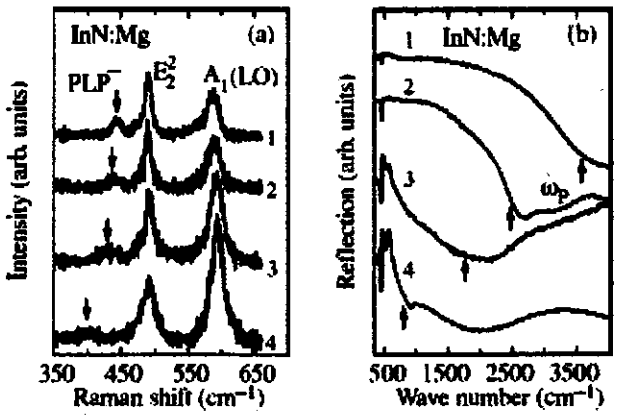

FIG. 27. (a) Raman spectra and (b) IR reflectivity spectra for InN:Mg epilayer with different carrier concentrations: $1-2\times10^{20}$ cm^{-3}; $2-1\times10^{19}$ cm^{-3}; $3-5\times10^{19}$ cm^{-3}; $4-1\times10^{19}$ cm^{-3} (Ref. 200).

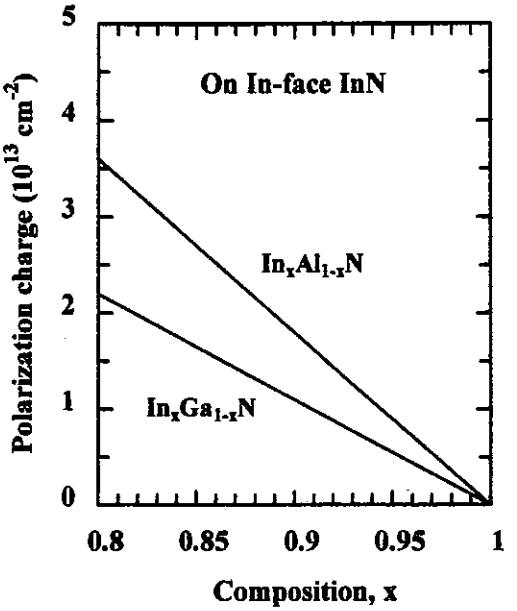

FIG. 28. Charge density in InN produced by InGaN and InAlN in the range of In mole fraction expected to be useful for heterojunctions with InN (Ref. 56).

non mode ν (in cm^{-1}) varied with strain ε (in %) as $\nu = 50\varepsilon + 481.5$.[203] Residual strain in the InN layer could be evaluated using this empirical formula. Mamutin *et al.* showed that by using different excitation energies, it is possible to test the InN layer at different depths.[174] They observed a strong additional band in the Raman spectrum for the lower excitation energy. This band is due to defect-induced Raman scattering and shows that the defect density dramatically rises with a distance from the surface of the film.

It has been demonstrated that the growth of less stable cubic ZB structure is also feasible. The ZB crystal structure belongs to the space group T_d^2, and the group theory analysis predicts one Raman active mode of F_2 representation: it is a polar mode which splits into the TO and LO components. There are very few reports existing on the measurement (experimental and theoretical) of phonon frequencies of cubic InN. Tabata *et al.* determined the experimental phonon frequencies of cubic InN grown by PA-MBE, the TO at 457, and the LO at 588 cm^{-1}.[162] They also calculated the TO phonon frequency of c-InN, and found a good agreement between theory and experiment. Later, Kaczmarczyk *et al.* also carried out the Raman scattering experiment and calculation for cubic InN grown by PA-MBE.[202] The TO and LO modes of cubic InN were found at 470 and 586 cm^{-1}. These values are in good agreement with their calculated values. While the LO frequency of Kaczmarczyk *et al.* agrees with the values reported by Tabata *et al.*, the TO phonon differs considerably. Tabata *et al.* excited their spectra above band gap (nonresonant spectra), and assigned a feature at 458 cm^{-1} to the TO phonon of cubic InN, which is similar to the second-order spectra of InAs, making it difficult to assign the TO of InN.

VII. PROGRESS TOWARDS InN BASED DEVICES

The latest progress in improving the InN film quality indicates that the InN film itself almost meets the requirements for application to practical devices. It is expected to be a highly promising material for the fabrication of high performance high electron mobility transistor (HEMT). InN as a HEMT channel requires a larger band gap barrier to induce and confine electrons. The probable choices of barriers are GaN or AlN or their alloys with InN, InGaN, or InAlN. The significant lattice mismatch between InN and GaN or AlN can result in a large piezo-electric charge, which is very advantageous for HEMT applications. The strained InGaN or InAlN is also a good choice as a barrier layer. Since the lattice constants of AlN and GaN are similarly larger than InN, there would only be a slight critical advantage to using InGaN as a surface barrier on InN. InAlN with a higher band gap than InGaN for the same In mole fraction, might also be expected to provide a higher Schottky barrier height, and higher breakdown field. AlInN is also expected to produce and confine a higher channel electron density than GaInN. When $In_xAl_{1-x}N$ or $In_xAGa_{1-x}N$ is grown on In-face InN, there will be a polarization-induced 2DEG formed in InN at the interface. Both a spontaneous polarization contribution and piezoelectric polarization contribution occur. Figure 28 shows a comparison between charge in InN produced by InGaN and InAlN in the range of In mole fraction expected to be useful.[56] A larger conduction band discontinuity, E_c, results in better electron confinement and allows for a higher sheet charge density in the well at the heterointerface. In order to realize InN-based HEMT, a suitable barrier layer is needed to grow on the InN channel layer, as explained above. Therefore, the development of growth process of the above-mentioned probable barriers compatible to that of InN will be required.

Kubota *et al.* prepared the multilayered film of (GaN/InN) for the first time by rf-magnetron sputtering.[46] However, they observed broad spectral profile from the GaN on InN, most likely due to interface diffusion in the InN surface due to the difference of the epitaxial growth temperature. Keller *et al.* investigated the flow modulation epitaxy of InN/GaN single and double heterostructures towards the fabrication of InN based HEMTs.[55] Growth process of GaN com-

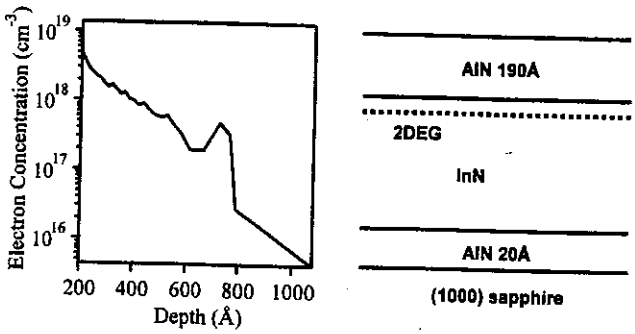

FIG. 29. $C-V$ profile of AlN/InN heterojunction showing 2DEG in InN (Ref. 56).

patible to that of InN has been studied. Thin InN and GaN layers could be deposited in a step flow growth mode using pulsed or alternative precursor injection scheme at growth temperature around 600 °C. Smooth surfaces of 3 nm GaN/(0.5–2) nm InN/2 μm S·I· GaN double heterostructures were obtained. However, structural defects were also formed during deposition of the GaN cap layer. Possibly, the InN islands grown on GaN are partially relaxed, resulting in defect formation during the deposition of the GaN cap layer due to the large lattice mismatch between InN and GaN (~10%). Similar observations had been made for InN quantum dots deposited by MBE.[55] The InN layer obviously intermixed with the GaN during GaN cap layer growth. Hall measurements revealed extremely high sheet carrier density (n_s) for these heterostructures. For an InN thickness of about 0.5 and 10 nm, n_s values of 2.6 and 3.3×10^{13} cm^{-2} were measured. The corresponding electron mobility values varied between 180 and 220 cm^2/V s. Due to the extremely high carrier concentration in combination with the low thickness of the InN channel, the carriers are not confined in the channel and spill over into the GaN layer. The measured electron mobility should then correspond to the conduction of electrons in GaN. Therefore, for the device applications the residual impurity concentration in the InN layer needs to be further reduced and successful deposition of InN containing heterostructure with preventing intermixing and strain related degradation of the film quality.

Schaff *et al.* obtained an electron density down to lower 10^{18} cm^{-3} in InN films and showed the evidence of 2DEG accumulation in InN.[56] They attempted to grow a AlInN/InN heterostructure with an In mole fraction between 80% and 90%. However, x-ray measurement showed that the incorporation of In was much lower than those predicted, most likely due to In segregation on the growing surface. Aluminum will incorporate preferently, and In will be squeezed out to the surface. As an alternative to AlInN, AlN has been used as an electron supply layer, and the hetorostructure is shown in Fig. 29. AlN would be expected to be fully relaxed which would remove the piezoelectric component of electrons from the 2DEG. Polarization induced charge, along with electrons from undoped InN can accumulate to form a 2DEG in InN under the AlN interface. The capacitance–voltage ($C-V$) profile from such a structure is seen in Fig. 29.[56] The profile is very similar to those seen for AlGaN/GaN 2DEG structures. This is the evidence of 2DEG accumulation seen in InN. The same group also observed very low leakage current and weak rectifying behavior in the first study on InN-based FET structures.[57] Amorphous AlN was used as the barrier material, which was prepared by MEE at low growth temperature. It was found that the surface morphology is improved after an AlN barrier layer is added to InN. Fabrication of InN based heterostructures and devices will shortly be expected. However, further improvement of electrical properties in the InN layer and development of growth technology of the barrier layers compatible to that of InN are still a great challenge.

The reported band gap value of InN is about 0.7 eV, which is compatible with the wavelength of the optical fiber. Therefore, another very important potential application of InN, fabrication of high-speed LD and PD in the optical communication system, is expected to happen. To realize such devices obtaining p-type InN is essential. As discussed, as-grown InN is always n type, and still InN could not be doped p type. Therefore, participation in this subject is very interesting.

VIII. SUMMARY AND CONCLUDING REMARKS

Initial synthesis of InN was in the form of powder or small crystal grown by using the interaction of indium compound with ammonia or thermal decomposition of the complex compound containing In and N. Considerable research on the growth of InN was done in the 1970s and 1980s, mainly by using reactive sputtering growth techniques. Single crystalline InN film has also been grown by the sputtering technique, however, the film qualities are very poor and has universally high carrier concentration near 10^{20} cm^{-3} and constantly low electron mobility of less than 100 cm^2/V s, except for the report of Tansley and Foley. There has been no report of such high mobility or low carrier concentration even by more popular growth techniques, such as MBE and MOVPE.

Even after the MOVPE and MBE techniques became available, difficulties in the growth of InN persisted. The major obstacles were the low InN dissociation temperature and high equilibrium N_2 vapor pressure over the InN film, and lack of suitable substrate. Due to the low InN dissociation temperature and high equilibrium N_2 vapor pressure over the InN film, the preparation of InN requires a low growth temperature. This creates a problem, in particular in conventional MOVPE systems, the most widely utilized deposition method for both research and device fabrication. In the MOVPE technique, to overcome the high kinetic barrier for the ammonia decomposition, a high growth temperature is required to obtain good quality film. Therefore, to produce reactive nitrogen radicals Wakahara *et al.* used plasma-assisted MOVPE and successfully grew the single crystalline InN film. They reported that without plasma assistance InN growth was not possible and dominated by metallic In formation. However, Matsuoka *et al.* successfully grew single crystalline InN by conventional MOVPE without any plasma assistance in the early days. The epitaxial growth of single crystalline and good quality InN film was widely explored and studied in the 1990s by using the modern

growth techniques, MOVPE and MBE, as well as by other growth techniques.

So far, sapphire is the most widely used as a substrate material. At the beginning, the InN film quality grown on sapphire substrate was poor, due large lattice mismatch and thermal expansion coefficient difference. However, researchers have revealed that the substrate surface pretreatment and insert of an intermediate buffer layer between substrate and epilayer can significantly improve the film quality. Nitridation of the sapphire substrate surface significantly improves the crystalline quality of InN as a result of the formation of AlN, and the quality of the InN film is strongly influenced by the nitridation condition. Some other substrates have also been used for the epitaxial growth of InN. Among them, considerable research was done on GaAs and GaP as a suitable semiconductor substrate with smaller lattice and thermal mismatch.

The electrical properties in the grown InN film until the 1999 were poor and became the focus of InN research. Electron concentrations below 10^{19} cm^{-3} were not reported until 1999 in single crystalline films; concentrations below 10^{20} cm^{-3} were rare while the maximum mobility was around 300 $cm^2/V\,s$. A breakthrough came from Yamaguchi *et al.* of Meijo University with a maximum mobility of 700 $cm^2/V\,s$, however, the carrier concentration was still high. The electron concentration down to lower 10^{18} cm^{-3} was achieved by Lu *et al.* of Cornell University in 2000 using MEE, and subsequently reported better film with a high electron mobility by conventional MBE. In fact, their work was a major break through to improve electrical properties in the grown InN film. Recently, a remarkable improvement in the growth of InN film has been revealed by MOVPE and MBE. High quality InN film with 2D growth and high growth rate can easily be obtained by MOVPE and MBE. The highest reported mobility and lowest background carrier concentration in the MOVPE grown InN film are 730 $cm^2/V\,s$ and 5.8×10^{18} cm^{-3}, respectively; while the highest reported mobility in the MBE grown thick InN film is 2050 $cm^2/V\,s$ and the lowest background carrier concentration is 3.49×10^{17} cm^{-3}, which are better than the MOVPE InN film. In spite of the relatively slow start, the MBE technique has made essential and faster progress in improving the InN film quality compared with MOVPE. The recent progress of the electrical properties in the MBE InN has brought about improvement of the buffer layer technique as well as selection of a suitable underlying layer.

Observation of photoluminescence in InN films had never been reported until 2001. It was thought that the grown InN film quality is too poor for photon emission. Most of the InN band gap studies were carried out by optical absorption and obtained a band gap about 1.9 eV. With the realization of high quality InN film several groups studied the PL measurement in the single crystalline InN film. Very recently many groups reported that the band gap energy of InN is much smaller than 1.89 eV. They also reported the band gap energy of InN to be around 0.65–0.90 eV, which created an exciting conflict and ambiguity about the exact band gap of InN. According to these groups, the previous studies were carried out in the poor quality InN film and the film was contaminated by oxygen, and therefore, showed a high band gap energy value than the real one. However, some others believe that the band gap of InN is around 1.89 eV as reported before, and the narrow band gap reported recently may be due to defect level emission, like yellow level emission of GaN. The current progress in this matter seems to lead to the conclusion that the optical band gap energy of InN is near about 0.7 eV.

The progress in the development of InN based heterostructures and devices is at the initial stage. However, the progress in improving the InN film quality indicates that the InN film itself almost approaches the application practical devices. Growth of a suitable barrier or cap layer on the InN layer is found to be difficult due to intermixing and interdiffusion into the InN layer. Schaff *et al.* of Cornell University, however, obtained an AlN barrier layer on the grown InN film and showed evidence of 2DEG accumulation in InN layer. The same group also observed very low leakage current and weak rectifying behavior in the first study on InN-based FET structure.

InN is still a less studied material compared with other compounds and there are many areas where further research is required. Also many properties of InN are yet to be established clearly as there are many ambiguities related to them. In order to improve the grown film quality and to settle the ambiguous properties of InN, more efforts in the growth and characterization of InN are very important. Still it has not been possible to grow InN layer free from the background. The highest mobility obtained in InN is smaller than the calculated value. Therefore, further improvement in electrical properties of the InN is one of the great challenges. Optical properties of InN are a most interesting problem in very recent years and a drastic change in the band gap energy that is the most fundamental optical property has been reported. The cause of the band gap narrowing from 1.9 to 0.7 eV is not so clear at the present stage, although several ideas such as an inclusion effect of the oxygen or the Burstein–Moss shift have already been proposed. Therefore, more studies should be carried out for clear understanding and to settle the real band gap energy of InN. One of the next challenges of InN research is to reduce crystalline defects like dislocations, point defects, etc., which will be very essential for high performance devices. These types of crystalline defects are caused both by the lattice and thermal mismatch as well as with experimental condition. It is important to find a suitable semiconductor substrate with good lattice and thermal match. MOVPE is the most extensively used growth technique for both research and device fabrication. Therefore, more effort in improving the MOVPE InN film quality is also very important. It is yet to be determined whether other growth methods, e.g., laser deposition, will become important. Another very important potential application of InN, fabrication of high-speed LD and PD in the optical communication system, is expected, as the reported band gap value of about 0.7 eV is compatible with the wavelength of the optical fiber. To realize such devices obtaining p type is essential. However, InN still cannot be doped p type because of high background donors. More work on this subject is essential.

[1] See, for example, the recent reviews and also the references in S. C. Jain, M. Willander, J. Narayan, and R. V. Overstraeten, J. Appl. Phys. **87**, 965 (2000); S. J. Pearton, J. C. Zolper, R. J. Shul, and F. Ren, *ibid.* **86**, 1 (1999).
[2] S. Strite and H. Morkoc, J. Vac. Sci. Technol. B **10**, 1237 (1992).
[3] S. N. Mohammad and H. Morkoc, Prog. Quantum Electron. **20**, 361 (1996).
[4] For a recent review, see, O. Ambacher, J. Phys. D **31**, 2653 (1998).
[5] I. Akasaki, H. Amano, N. Koide, M. Kotaki, and K. Manabe, Physica B **185**, 428 (1993).
[6] S. Nakamura, M. Senoh, and T. Mukai, Jpn. J. Appl. Phys., Part 2 **32**, L8 (1993).
[7] S. Nakamura, M. Senoh, S. Nagahama, N. Iwasa, T. Yamada, T. Matsushita, H. Kiyoku, and Y. Sugimoto, Jpn. J. Appl. Phys., Part 2 **35**, L74 (1996).
[8] V. W. L. Chin, T. L. Tansley, and T. Osotchan, J. Appl. Phys. **75**, 7365 (1994).
[9] S. K. O'Leary, B. E. Foutz, M. S. Shur, U. V. Bhapkar, and L. F. Eastman, J. Appl. Phys. **83**, 826 (1998).
[10] E. Bellotti, B. K. Doshi, K. F. Brennan, J. D. Albrecht, and P. P. Ruden, J. Appl. Phys. **85**, 916 (1999).
[11] B. E. Foutz, S. K. O'Leary, M. S. Shur, and L. F. Eastman, J. Appl. Phys. **85**, 7727 (1999).
[12] T. L. Tansley and C. P. Foley, J. Appl. Phys. **59**, 3241 (1986).
[13] A. Yamamoto, M. Tsujino, M. Ohkubo, and A. Hashimoto, Sol. Energy Mater. Sol. Cells **35**, 53 (1994).
[14] Z. G. Qian, W. Z. Shen, H. Ogawa, and Q. X. Guo, J. Appl. Phys. **92**, 3683 (2002).
[15] V. Y. Davydov *et al.*, Phys. Status Solidi B **229**, R1 (2002).
[16] V. Y. Davydov *et al.*, Phys. Status Solidi B **230**, R4 (2002).
[17] J. Wu, W. Walukiewicz, K. M. Yu, J. W. Ager III, E. E. Haller, H. Lu, W. J. Schaff, Y. Saito, and Y. Nanishi, Appl. Phys. Lett. **80**, 3967 (2002).
[18] T. Matsuoka, H. Okamoto, M. Nakao, H. Harima, and E. Kurimoto, Appl. Phys. Lett. **81**, 1246 (2002).
[19] M. Hori, K. Kano, T. Yamaguchi, Y. Saito, T. Araki, Y. Nanishi, N. Teraguchi, and A. Suzuki, Phys. Status Solidi B **234**, 750 (2002).
[20] V. Y. Davydov *et al.*, Phys. Status Solidi B **234**, 787 (2002).
[21] Y. Saito, H. Harima, E. Kurimoto, T. Yamaguchi, N. Teraguchi, A. Suzuki, T. Araki, and Y. Nanishi, Phys. Status Solidi B **234**, 796 (2002).
[22] T. Miyajima *et al.*, Phys. Status Solidi B **234**, 801 (2002).
[23] R. Juza and H. Hahn, Z. Anorg. Allg. Chem. **239**, 282 (1938).
[24] R. Juza and A. Rabenau, Z. Anorg. Allg. Chem. **285**, 212 (1956).
[25] T. Renner, Z. Anorg. Allg. Chem. **298**, 28 (1958).
[26] J. Pastrnak and L. Souckova, Phys. Status Solidi **3**, K71 (1963).
[27] G. V. Samsonov, Nitridy Kiev, 1969.
[28] N. A. Gorjunova, Slosnye Almazopodobnye Poluprovodniki, Moscow, 1964.
[29] J. B. McChesney, P. M. Bridenbaugh, and P. B. O'Connor, Mater. Res. Bull. **5**, 783 (1970).
[30] H. J. Hovel and J. J. Cuomo, Appl. Phys. Lett. **20**, 71 (1972).
[31] J. W. Trainor and K. Rose, J. Electron. Mater. **3**, 821 (1974).
[32] A. F. Andreeyva and O. J. Eliseejva, Z. Neorg. Chim. **13**, 185 (1974).
[33] K. Osamura, K. Nakajima, Y. Murakami, H. P. Shingu, and A. Ohtsuki, Solid State Commun. **11**, 617 (1972).
[34] K. Osamura, S. Naka, and Y. Murakami, J. Appl. Phys. **46**, 3432 (1975).
[35] N. Puychevrier and M. Menoret, Thin Solid Films **36**, 141 (1976).
[36] L. A. Marasina, I. G. Pichugin, and M. Tlaczala, Krist. Tech. **12**, 541 (1977).
[37] B. R. Natarajan, A. H. Eltoukhy, J. E. Greene, and T. L. Barr, Thin Solid Films **69**, 201 (1980).
[38] T. L. Tansley and C. P. Foley, Electron. Lett. **20**, 1066 (1984).
[39] C. P. Foley and T. L. Tansley, Appl. Surf. Sci. **22/23**, 663 (1985).
[40] T. L. Tansley and C. P. Foley, in Proceedings of the 3rd International Conference on Semi-Insulating III-V Materials, Warm Springs, Oregon, 1984, p. 497.
[41] C. P. Foley and T. L. Tansley, Phys. Rev. B **33**, 1430 (1986).
[42] T. L. Tansley and C. P. Foley, J. Appl. Phys. **60**, 2092 (1986).
[43] C. P. Foley and J. Lyngdal, J. Vac. Sci. Technol. A **5**, 1708 (1987).
[44] K. L. Westra, R. P. W. Lawson, and M. J. Brett, J. Vac. Sci. Technol. A **6**, 1730 (1988).
[45] B. T. Sullivan, R. R. Parsons, K. L. Westra, and M. J. Brett, J. Appl. Phys. **64**, 4144 (1988).
[46] K. Kubota, Y. Kobayashi, and K. Fujimoto, J. Appl. Phys. **66**, 2984 (1989).
[47] Y. Sato and S. Sato, Jpn. J. Appl. Phys., Part 2 **28**, L1641 (1989).
[48] T. Matsuoka, H. Tanaka, T. Sasaki, and A. Katsui, *Proceedings of the Sixteenth International Symposium on GaAs and Related Compounds, Karuizawa, Japan*, September 25–29, 1989 (Institute of Physics, Bristol, 1990), p. 141.
[49] A. Wakahara and A. Yoshida, Appl. Phys. Lett. **54**, 709 (1989).
[50] A. Wakahara, T. Tsuchiya, and A. Yoshida, J. Cryst. Growth **99**, 385 (1990).
[51] A. Yamamoto, T. Tanaka, K. Koide, and A. Hashimoto, Phys. Status Solidi A **194**, 510 (2002).
[52] H. Lu, W. J. Schaff, L. F. Eastman, J. Wu, W. Walukiewicz, K. M. Yu, J. W. Auger III, E. E. Haller, and O. Ambacher, Abstract of the 44th Electronic Material Conference, Santa Barbara, CA, June 26–28, 2002; J. Electron. Mater. (to be published); W. J. Schaff (private communication, Cornell University, Ithaca, N.Y.).
[53] T. Yodo, H. Ando, D. Nosei, and Y. Harada, Phys. Status Solidi B **228**, 21 (2001).
[54] T. Yodo, H. Yona, H. Ando, D. Nosei, and Y. Harada, Appl. Phys. Lett. **80**, 968 (2002).
[55] S. Keller, I. Ben-yaacov, S. P. Denvers, and U. K. Mishra, Proceedings of the International Workshop on Nitride Semiconductors (IWN' 2000), Nagoya, Japan, September 24–27, 2000, IPAP conference series 1, p. 233.
[56] W. J. Schaff, H. Lu, J. Hwang, and H. Wu, Proceedings of the Seventeenth Biennial IEEE/Cornell Conference on Advanced Concepts in High Performance Devices, August 7–9, 2000, p. 225.
[57] H. Lu, W. J. Schaff, L. F. Eastman, and C. Wood, Mater. Res. Soc. Symp. Proc. **693**, 9 (2002).
[58] O. Ambacher, M. S. Brandt, R. Dimitrov, T. Metzger, M. Stutzmann, R. A. Fischer, A. Miehr, A. Bergmajer, and G. Dollinger, J. Vac. Sci. Technol. B **14**, 3532 (1996).
[59] A. Koukitu, N. Takahashi, and H. Seki, Jpn. J. Appl. Phys., Part 2 **36**, L1136 (1997).
[60] T. Matsuoka, in *GaN and Related Materials*, edited by S. J. Pearton (Gordon and Breach, New York, 1997), pp. 53–59.
[61] A. Koukitu, T. Taki, N. Takahashi, and H. Seki, J. Cryst. Growth **197**, 99 (1999).
[62] A. Koukitu, Y. Kumagai, N. Kubota, and H. Seki, Phys. Status Solidi B **216**, 707 (1999).
[63] A. Yamamoto, Y. Murakami, K. Koide, M. Adachi, and A. Hashimoto, Phys. Status Solidi B **228**, 5 (2001).
[64] W. K. Chen, Y. C. Pan, H. C. Lin, J. Ou, W. H. Chen, and M. C. Lee, Jpn. J. Appl. Phys., Part 2 **36**, L1625 (1997).
[65] M. Adachi, Y. Murakami, A. Hashimoto, and A. Yamamoto, Proceedings of the International Workshop on Nitride Semiconductors (IWN' 2000), Nagoya, Japan, September 24–27, 2000, IPAP conference series 1, p. 339.
[66] A. Yamamoto, T. Shin-ya, T. Sugiura, and A. Hashimoto, J. Cryst. Growth **189/190**, 461 (1998).
[67] A. Yamamoto, T. Tanaka, K. Koide, and A. Hashimoto, Phys. Status Solidi A **194**, 510 (2002).
[68] S. Nakamura, Y. Harada, and M. Seno, Appl. Phys. Lett. **58**, 2021 (1991).
[69] K. Nishida, S. Haneda, K. Hara, H. Munekata, and H. Kukimoto, J. Cryst. Growth **170**, 312 (1997).
[70] C.-C. Yang, G.-C. Chi, C.-K. Huang, and M.-C. Wu, J. Cryst. Growth **200**, 32 (1999).
[71] A. Yamamoto, M. Adachi, and A. Hashimoto, J. Cryst. Growth **230**, 351 (2001).
[72] F.-H. Yang, J.-S. Hwang, Y.-J. Yang, K.-H. Chen, and J.-H. Wang, Jpn. J. Appl. Phys., Part 2 **41**, L1321 (2002).
[73] Q. Fareed, J. Yang, J. Zhang, V. Adivarahan, and M. A. Khan, Proceedings of the International Workshop on Nitride Semiconductors (IWN' 2000), Nagoya, Japan, September 24–27, 2000, IPAP conference series 1, p. 237.
[74] Q. Guo, O. Kato, and A. Yoshida, J. Appl. Phys. **73**, 7969 (1993).
[75] Q. Guo and A. Yoshida, Jpn. J. Appl. Phys., Part 1 **33**, 90 (1994).
[76] Q. Guo and A. Yoshida, Jpn. J. Appl. Phys., Part 1 **33**, 2453 (1994).
[77] Q. Guo, T. Yamamura, A. Yoshida, and N. Itoh, J. Appl. Phys. **75**, 4927 (1994).
[78] Q. Guo, H. Ogawa, H. Yamano, and A. Yoshida, Appl. Phys. Lett. **66**, 715 (1995).
[79] H.-J. Kwon, Y.-H. Lee, O. Miki, H. Yamano, and A. Yoshida, Appl. Phys. Lett. **69**, 937 (1996).
[80] M. Sato, Jpn. J. Appl. Phys., Part 2 **36**, L595 (1997).

[81] M. Sato, Jpn. J. Appl. Phys., Part 2 **36**, L658 (1997).
[82] Q. X. Guo, M. Nishio, H. Ogawa, A. Wakahara, and A. Yoshida, Phys. Rev. B **58**, 15304 (1998).
[83] T. Tsuchiya, H. Yamano, O. Miki, A. Wakahara, and A. Yoshida, Jpn. J. Appl. Phys., Part 1 **38**, 1884 (1999).
[84] T. Tsuchiya, O. Miki, K. Shimada, M. Ohnishi, A. Wakahara, and A. Yoshida, J. Cryst. Growth **220**, 185 (2000).
[85] T. Tsuchiya, M. Ohnishi, A. Wakahara, and A. Yoshida, J. Cryst. Growth **220**, 191 (2000).
[86] X. Li, B. Zhou, K. S. A. Butcher, E. Florido, N. Syakir, and T. L. Tansley, Proceedings of the Australian Compound Optoelectronic Materials Devices Conference, Sydney, Australia, December 12–14, 1994, p. 43.
[87] A. G. Bhuiyan, T. Tanaka, A. Yamamoto, and A. Hashimoto, Phys. Status Solidi A **194**, 502 (2002).
[88] A. G. Bhuiyan, T. Tanaka, K. Kasashima, A. Hashimoto, and A. Yamamoto, 5th International Conference on Nitride Semiconductors (ICNS-5), Nara, Japan, May 25–30, 2003 (accepted).
[89] R. F. Davis, M. J. Paisley, Z. Sitar, D. J. Kester, K. S. Ailey, K. Linthicum, L. B. Rowland, S. Tanaka, and R. S. Kern, J. Cryst. Growth **178**, 87 (1997).
[90] C. R. Abernathy, J. D. MacKenzie, and S. M. Donovan, J. Cryst. Growth **178**, 74 (1997).
[91] W. C. Hughes, W. H. Rowland, Jr., M. A. L. Johnson, S. Fujita, J. W. Cook, Jr., J. F. Schetzina, J. Ren, and J. A. Edmond, J. Vac. Sci. Technol. B **13**, 1571 (1995).
[92] R. C. Powell, N. E. Lee, Y. W. Kim, and J. E. Greene, J. Appl. Phys. **73**, 189 (1993).
[93] A. Botchkarev, A. Salvador, B. Sverdlov, J. Myoung, and H. Morkoc, J. Appl. Phys. **77**, 4455 (1995).
[94] R. J. Molnar and T. D. Moustakas, J. Appl. Phys. **76**, 4587 (1994).
[95] K. Iwata, H. Asahi, S. J. Yu, K. Asami, H. Fujita, M. Fushida, and S. Gonda, Jpn. J. Appl. Phys., Part 2 **35**, L289 (1996).
[96] W. E. Hoke, P. J. Lemonias, and D. G. Weir, J. Cryst. Growth **111**, 1024 (1991).
[97] N. E. Lee, R. C. Powell, Y. W. Kim, and J. E. Greene, J. Vac. Sci. Technol. A **13**, 2293 (1995).
[98] Z. Yang, L. K. Li, and W. I. Wang, Appl. Phys. Lett. **67**, 1686 (1995).
[99] N. Grandjean, J. Massies, and M. Leroux, Appl. Phys. Lett. **69**, 2071 (1996).
[100] W. Kim, A. Salvador, A. E. Botchkarev, O. Aktas, S. N. Mohammad, and H. Morkoc, Appl. Phys. Lett. **69**, 559 (1996).
[101] M. Kamp, M. Mayer, A. Pelzmann, and K. J. Ebeling, Mater. Res. Soc. Symp. Proc. **449**, 161 (1997).
[102] H. Okumura, S. Yoshida, and E. Sakuma, J. Cryst. Growth **120**, 114 (1991).
[103] A. Koukitu and H. Seki, Jpn. J. Appl. Phys., Part 2 **36**, L750 (1997).
[104] A. Koukitu, N. Takahashi, T. Taki, and H. Seki, Jpn. J. Appl. Phys., Part 2 **35**, L673 (1996).
[105] Y. F. Ng, Y. G. Cao, M. H. Xie, X. L. Wang, and S. Y. Tong, Appl. Phys. Lett. **81**, 3960 (2002).
[106] C. Nörenberg, M. G. Martin, R. A. Oliver, M. R. Castell, and G. A. D. Briggs, J. Phys. D **35**, 615 (2002).
[107] C. Nörenberg, R. A. Oliver, M. G. Martin, L. Allers, M. R. Castell, and G. A. D. Briggs, Phys. Status Solidi A **194**, 536 (2002).
[108] H. Lu, W. J. Schaff, J. Hwang, H. Wu, W. Yeo, A. Pharkya, and L. Eastman, Appl. Phys. Lett. **77**, 2548 (2000).
[109] Y. Saito, H. Harima, E. Kurimoto, T. Yamaguchi, N. Teraguchi, A. Suzuki, T. Araki, and Y. Nanishi, Phys. Status Solidi B **234**, 796 (2002).
[110] T. Yamaguchi, Y. Saito, K. Kano, T. Araki, N. Teraguchi, A. Suzuki, and Y. Nanishi, Phys. Status Solidi B **228**, 17 (2001).
[111] Y. Saito, Y. Tanabe, T. Yamaguchi, N. Teraguchi, A. Suzuki, T. Araki, and Y. Nanishi, Phys. Status Solidi B **228**, 13 (2001).
[112] K. Xu, W. Terashima, T. Hata, N. Hashimoto, Y. Ishitani, and A. Yoshikawa, Phys. Status Solidi C **0**, 377 (2002).
[113] C. R. Abernathy, S. J. Pearton, F. Ren, and P. W. Wisk, J. Vac. Sci. Technol. B **11**, 179 (1993).
[114] J. Aderhold, V. Yu. Davydov, F. Fedler, H. Klausing, D. Mistele, T. Rotter, O. Semchinova, J. Stemmer, and J. Graul, J. Cryst. Growth **222**, 701 (2001).
[115] W. A. Bryden, J. S. Morgan, T. J. Kistenmacher, D. Dayan, R. Fainchtein, and T. O. Poehler, Mater. Res. Soc. Symp. Proc. **162**, 567 (1990).
[116] T. J. Kistenmacher, D. Dayan, R. Fainchtein, W. A. Bryden, J. S. Morgan, and T. O. Poehler, Mater. Res. Soc. Symp. Proc. **162**, 573 (1990).
[117] J. S. Morgan, T. J. Kistenmacher, W. A. Bryden, and T. O. Poehler, Mater. Res. Soc. Symp. Proc. **162**, 579 (1990).
[118] T. J. Kistenmacher, W. A. Bryden, J. S. Morgan, and T. O. Poehler, J. Appl. Phys. **68**, 1541 (1990).
[119] T. J. Kistenmacher and W. A. Bryden, Appl. Phys. Lett. **59**, 1844 (1991).
[120] J. S. Morgan, T. J. Kistenmacher, W. A. Bryden, and S. A. Ecelberger, Mater. Res. Soc. Symp. Proc. **202**, 383 (1991).
[121] T. L. Tansley and R. J. Egan, Phys. Rev. B **45**, 10942 (1992).
[122] T. L. Tansley and R. J. Egan, Mater. Res. Soc. Symp. Proc. **242**, 395 (1992).
[123] W. A. Bryden, S. A. Ecelberger, J. S. Morgan, T. O. Poehler, and T. J. Kistenmacher, Mater. Res. Soc. Symp. Proc. **242**, 409 (1992).
[124] T. J. Kistenmacher, S. A. Ecelberger, and W. A. Bryden, Mater. Res. Soc. Symp. Proc. **242**, 441 (1992).
[125] T. J. Kistenmacher and W. A. Bryden, Appl. Phys. Lett. **62**, 1221 (1993).
[126] T. J. Kistenmacher, S. A. Ecelberger, and W. A. Bryden, J. Appl. Phys. **74**, 1684 (1993).
[127] W. A. Bryden, S. A. Ecelberger, and T. J. Kistenmacher, Appl. Phys. Lett. **64**, 2864 (1994).
[128] Q. X. Guo, N. Shingai, M. Nishio, and H. Ogawa, J. Cryst. Growth **189/190**, 466 (1998).
[129] Q. X. Guo, M. Nishio, H. Ogawa, and A. Yoshida, Jpn. J. Appl. Phys., Part 2 **38**, L490 (1999).
[130] Q. X. Guo, A. Okade, H. Kidera, T. Tanaka, M. Nishio, and H. Ogawa, J. Cryst. Growth **237–239**, 1032 (2002).
[131] I. J. Lee, J. W. Kim, T.-B. Hur, Y.-H. Hwang, and H.-K. Kim, Appl. Phys. Lett. **81**, 475 (2002).
[132] H. F. Yang, W. Z. Shen, Z. G. Qian, Q. J. Pan, H. Ogawa, and Q. X. Guo, J. Appl. Phys. **91**, 9803 (2002).
[133] I. J. Lee, J. W. Kim, Y.-H. Hwang, and H.-K. Kim, J. Appl. Phys. **92**, 5814 (2002).
[134] Motlan, E. M. Goldys, and T. L. Tansley, J. Cryst. Growth **241**, 165 (2002).
[135] K. S. A. Butcher, M. Wintrebert-Fouquet, P. P.-T. Chen, T. L. Tansley, and S. Srikeaw, Mater. Res. Soc. Symp. Proc. **693**, 341 (2002).
[136] K. S. A. Butcher, H. Dou, E. M. Goldys, T. L. Tansley, and S. Srikeaw, Phys. Status Solidi C **0**, 373 (2002).
[137] O. Igarashi, Jpn. J. Appl. Phys., Part 1 **31**, 2665 (1992).
[138] Y. Sato and S. Sato, J. Cryst. Growth **144**, 15 (1994).
[139] N. Takahashi, J. Ogasawara, and A. Koukitu, J. Cryst. Growth **172**, 298 (1997).
[140] N. Takahashi, R. Matsumoto, A. Koukitu, and H. Seki, Jpn. J. Appl. Phys., Part 2 **36**, L743 (1997).
[141] H. Sunakawa, A. Yamaguchi, A. Kimura, and A. Usui, Jpn. J. Appl. Phys., Part 2 **35**, L1395 (1996).
[142] R. D. Vispute, J. Narayan, H. Wu, and K. Jagannadham, J. Appl. Phys. **77**, 4724 (1995).
[143] R. D. Vispute, H. Wu, and J. Narayan, Appl. Phys. Lett. **67**, 1549 (1995).
[144] D. Feiler, R. S. Williams, A. A. Talin, H. Yoon, and M. S. Goorsky, J. Cryst. Growth **171**, 12 (1997).
[145] P. Bhattacharya, T. K. Sharma, S. Singh, A. Ingale, and L. M. Kukreja, J. Cryst. Growth **236**, 5 (2002).
[146] Y. Sato, S. Kakinuma, and S. Sato, Jpn. J. Appl. Phys., Part 1 **33**, 4377 (1994).
[147] Y. Sato and S. Sato, J. Cryst. Growth **146**, 262 (1995).
[148] I. Bello, W. M. Lau, R. P. W. Lawson, and K. K. Foo, J. Vac. Sci. Technol. A **10**, 1642 (1992).
[149] Y.-J. Bai, Z.-G. Liu, X.-G. Xu, D.-L. Cui, X.-P. Hao, X. Feng, and Q.-L. Wang, J. Cryst. Growth **241**, 189 (2002).
[150] A. Yamamoto, M. Tsujino, M. Ohkubo, and A. Hashimoto, J. Cryst. Growth **137**, 415 (1994).
[151] Y. C. Pan, W. H. Lee, C. K. Shu, H. C. Lin, C. I. Chiang, H. Chang, D. S. Lin, M. C. Lee, and W. K. Chen, Jpn. J. Appl. Phys., Part 1 **38**, 645 (1999).
[152] T. Tsuchiya, H. Yamano, O. Miki, A. Wakahara, and A. Yoshida, Jpn. J. Appl. Phys., Part 1 **38**, 1884 (1999).
[153] W. K. Chen, H. C. Lin, Y. C. Pan, J. Ou, C. K. Shu, W. H. Chen, and M. C. Lee, Jpn. J. Appl. Phys., Part 1 **37**, 4870 (1998).
[154] A. Yamamoto, Y. Yamauchi, T. Ogawa, M. Ohkubo, and A. Hashimoto, Inst. Phys. Conf. Ser. **142**, 879 (1996).
[155] A. Yamamoto, Y. Yamauchi, M. Ohkubo, A. Hashimoto, and T. Saitoh, Solid-State Electron. **41**, 149 (1997).
[156] S. Strite, D. Chandrasekhar, D. J. Smith, J. Sariel, H. Chen, N. Teraguchi, and H. Morkoc, J. Cryst. Growth **127**, 204 (1993).

[157] A. Yamamoto, Y. Yamauchi, M. Ohkubo, and A. Hashimoto, J. Cryst. Growth **174**, 641 (1997).
[158] A. Yamamoto, M. Adachi, T. Arita, T. Sugiura, and A. Hashimoto, Phys. Status Solidi A **176**, 595 (1999).
[159] M. Adachi, A. Seki, A. Hashimoto, and A. Yamamoto, Proceedings of the International Workshop on Nitride Semiconductors (IWN' 2000), Nagoya, Japan, September 24–27, 2000, IPAP conference series 1, p. 347.
[160] A. Yamamoto, T. Shin-ya, T. Sugiura, M. Ohkubo, and A. Hashimoto, J. Cryst. Growth **189/190**, 476 (1998).
[161] A. P. Lima, A. Tabata, J. R. Leite, S. Kaiser, D. Schikora, B. Schottker, T. Frey, D. J. As, and K. Lischka, J. Cryst. Growth **201/202**, 396 (1999).
[162] A. Tabata *et al.*, Appl. Phys. Lett. **74**, 362 (1999).
[163] A. G. Bhuiyan, A. Hashimoto, A. Yamamoto, and R. Ishigami, J. Cryst. Growth **212**, 379 (2000).
[164] A. G. Bhuiyan, A. Yamamoto, A. Hashimoto, and R. Ishigami, Proceedings of the International Workshop on Nitride Semiconductors (IWN' 2000), Nagoya, Japan, September 24–27, 2000, IPAP conference series 1, p. 343.
[165] A. G. Bhuiyan, A. Yamamoto, and A. Hashimoto, Phys. Status Solidi B **228**, 27 (2001).
[166] A. G. Bhuiyan, A. Yamamoto, A. Hashimoto, and Y. Ito, J. Cryst. Growth **236**, 59 (2002).
[167] J. S. Pan, A. T. S. Wee, C. H. A. Huan, H. S. Tan, and K. L. Tan, J. Phys. D **29**, 2997 (1996).
[168] H. Lu, W. J. Schaff, J. Hwang, H. Wu, G. Koley, and L. Eastman, Appl. Phys. Lett. **79**, 1489 (2001).
[169] S. Yamaguchi, M. Kariya, S. Nitta, T. Takeuchi, C. Wetzel, H. Amano, and I. Akasaki, J. Appl. Phys. **85**, 7682 (1999).
[170] J. H. M. Nicholls, H. Gallagher, B. Henderson, C. Trager-Cowan, P. G. Middleton, K. P. O'Donnel, T. S. Cheng, C. T. Foxon, and B. H. T. Chai, Mater. Res. Soc. Symp. Proc. **395**, 535 (1996).
[171] P. Kung, A. Saxler, X. Zhang, D. Walker, R. Lavado, and M. Razeghi, Appl. Phys. Lett. **69**, 2116 (1996).
[172] T. Ishi, Y. Tazoh, and S. Miyazawa, Mater. Res. Soc. Symp. Proc. **468**, 155 (1997).
[173] A. Brown *et al.*, J. Vac. Sci. Technol. B **16**, 1300 (1998).
[174] V. V. Mamutin *et al.*, Phys. Status Solidi A **176**, 247 (1999).
[175] Y. Saito, N. Teraguchi, A. Suzuki, and Y. Nanishi, Proceedings of the International Workshop on Nitride Semiconductors (IWN' 2000), Nagoya, Japan, September 24–27, 2000, IPAP conference series **1**, p. 182.
[176] Y. Saito, N. Teraguchi, A. Suzuki, T. Araki, and Y. Nanishi, Jpn. J. Appl. Phys., Part 2 **40**, L91 (2001).
[177] Y. Saito, T. Yamaguchi, H. Kanazawa, K. Kano, T. Araki, Y. Nanishi, A. Suzuki, and N. Teraguchi, J. Cryst. Growth **237–239**, 1017 (2002).
[178] M. Higashiwaki and T. Matsui, Jpn. J. Appl. Phys., Part 2 **41**, L540 (2002).
[179] M. Higashiwaki and T. Matsui, Phys. Status Solidi C **0**, 360 (2002).
[180] K. Kim, W. R. L. Lambrecht, and B. Segall, Phys. Rev. B **53**, 16310 (1996).
[181] A. Yamamoto, T. Tanaka, A. G. Bhuiyan, K. Sugita, K. Kasashima, Y. Kimura, A. Hashimoto, and V. Yu. Davydov, 5th International Conference on Nitride Semiconductors (ICNS-5), Nara, Japan, May 25–30, 2003 (accepted).
[182] D. C. Look, H. Lu, W. J. Schaff, J. Jasinski, and Z. Liliental-Weber, Appl. Phys. Lett. **80**, 258 (2002).
[183] M. Seelmann-Eggebert, J. L. Weher, H. Obloh, H. Zimmermann, A. Rar, and S. Porowski, Appl. Phys. Lett. **71**, 2635 (1997).
[184] See a recent review and also the references in that E. S. Hellman, MRS Internet J. Nitride Semicond. Res. **3**, 11 (1998).
[185] T. Onozu, I. Gunji, R. Miura, S. S. C. Ammal, M. Kubo, K. Teraishi, A. Miyamoto, Y. Iyechika, and T. Maeda, Jpn. J. Appl. Phys., Part 1 **38**, 2544 (1999).
[186] Q. Guo, O. Kato, and A. Yoshida, J. Electrochem. Soc. **139**, 2008 (1992).
[187] J. R. Mileham, S. J. Pearton, C. R. Abernathy, J. D. Mackenzie, R. J. Shul, and S. P. Kilcoyne, J. Vac. Sci. Technol. A **14**, 836 (1996).
[188] S. J. Pearton, C. R. Abernathy, F. Ren, J. R. Lothian, P. W. Wisk, and A. Katz, J. Vac. Sci. Technol. A **11**, 1772 (1993).
[189] M. Ohkubo and O. Takai, Proceedings of the International Workshop on Nitride Semiconductors (IWN' 2000), Nagoya, Japan, September 24–27, 2000, IPAP conference series 1, p. 770.
[190] S. J. Pearton, C. R. Abernathy, and F. Ren, Appl. Phys. Lett. **64**, 2294 (1994).
[191] R. J. Shul, C. G. Willison, M. M. Bridges, J. Han, J. W. Lee, S. J. Pearton, C. R. Abernathy, J. D. Mackenzie, and S. M. Donovan, Solid-State Electron. **42**, 2269 (1998).
[192] Q. Guo, M. Matsuse, M. Nishio, and H. Ogawa, Jpn. J. Appl. Phys., Part 1 **39**, 5048 (2000).
[193] D. W. Jenkins and J. D. Dow, Phys. Rev. B **39**, 3317 (1989).
[194] C. Stampfl, C. G. Van de Walle, D. Vogel, P. Kruger, and J. Pollmann, Phys. Rev. B **61**, R7846 (2000).
[195] V. V. Mamutin, V. A. Vekshin, V. Y. Davydov, V. V. Ratnikov, Y. A. Kudriavtsev, B. Y. Ber, V. V. Emtsev, and S. V. Ivanov, Phys. Status Solidi A **176**, 373 (1999).
[196] H. Lu, W. J. Schaff, J. Hwang, and L. F. Eastman, Mater. Res. Soc. Symp. Proc. **680E**, E3.2 (2001).
[197] T. Inushima, V. V. Mamutin, V. A. Vekshin, S. V. Ivanov, T. Sakon, M. Motokawa, and S. Ohoya, J. Cryst. Growth **227–228**, 481 (2001).
[198] J. S. Dyck, K. Kash, K. Kim, W. R. L. Lambrecht, C. C. Hayman, A. Argoitia, M. T. Grossner, W. L. Zhou, and J. C. Angus, Mater. Res. Soc. Symp. Proc. **482**, 549 (1998).
[199] T. Inushima, T. Shiraishi, V. Y. Davydov, Solid State Commun. **110**, 491 (1999).
[200] V. Y. Davydov *et al.*, Appl. Phys. Lett. **75**, 3297 (1999).
[201] V. Y. Davydov *et al.*, Phys. Status Solidi B **216**, 779 (1999).
[202] G. Kaczmarczyk *et al.*, Appl. Phys. Lett. **76**, 2122 (2000).
[203] E. Kurimoto, H. Harima, A. Hashimoto, and A. Yamamoto, Phys. Status Solidi B **228**, 1 (2001).